

RESEARCH ARTICLE

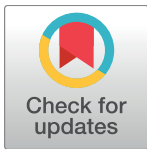
Divergent bornaviruses from Australian carpet pythons with neurological disease date the origin of extant *Bornaviridae* prior to the end-Cretaceous extinction

Timothy H. Hyndman¹*, Catherine M. Shilton², Mark D. Stenglein³, James F. X. Wellehan, Jr.⁴

1 College of Veterinary Medicine, School of Veterinary and Life Sciences, Murdoch University, Perth, Australia, **2** Berrimah Veterinary Laboratories, Department of Primary Industry and Resources, Northern Territory Government, Berrimah, Northern Territory, Australia, **3** Department of Microbiology, Immunology, and Pathology, College of Veterinary Medicine and Biomedical Sciences, Colorado State University, Fort Collins, Colorado, United States of America, **4** Department of Comparative, Diagnostic, and Population Medicine, College of Veterinary Medicine, University of Florida, Gainesville, Florida, United States of America

* These authors contributed equally to this work.

* t.hyndman@murdoch.edu.au



OPEN ACCESS

Citation: Hyndman TH, Shilton CM, Stenglein MD, Wellehan JFX, Jr. (2018) Divergent bornaviruses from Australian carpet pythons with neurological disease date the origin of extant *Bornaviridae* prior to the end-Cretaceous extinction. PLoS Pathog 14(2): e1006881. <https://doi.org/10.1371/journal.ppat.1006881>

Editor: Jens H. Kuhn, Division of Clinical Research, UNITED STATES

Received: September 12, 2017

Accepted: January 17, 2018

Published: February 20, 2018

Copyright: © 2018 Hyndman et al. This is an open access article distributed under the terms of the [Creative Commons Attribution License](https://creativecommons.org/licenses/by/4.0/), which permits unrestricted use, distribution, and reproduction in any medium, provided the original author and source are credited.

Data Availability Statement: Coding complete viral genome sequences are available in GenBank with accessions MF135780 and MF135781. Raw sequence data have been deposited in the NCBI Short Read Archive (SRA; accession PRJNA390668). Partial bornavirus polymerase gene sequences are available in GenBank with accessions MF166903-MF166917. All other relevant data are within the paper and its supporting information files.

Abstract

Tissue samples from Australian carpet pythons (*Morelia spilota*) with neurological disease were screened for viruses using next-generation sequencing. Coding complete genomes of two bornaviruses were identified with the gene order 3'-N-X-P-G-M-L, representing a transposition of the G and M genes compared to other bornaviruses and most mononegaviruses. Use of these viruses to search available vertebrate genomes enabled recognition of further endogenous bornavirus-like elements (EBLs) in diverse placental mammals, including humans. Codivergence patterns and shared integration sites revealed an ancestral laurasiatherian EBLG integration (77 million years ago [MYA]) and a previously identified afrotherian EBLG integration (83 MYA). The novel python bornaviruses clustered more closely with these EBLs than with other exogenous bornaviruses, suggesting that these viruses diverged from previously known bornaviruses prior to the end-Cretaceous (K-Pg) extinction, 66 MYA. It is possible that EBLs protected mammals from ancient bornaviral disease, providing a selective advantage in the recovery from the K-Pg extinction. A degenerate PCR primer set was developed to detect a highly conserved region of the bornaviral polymerase gene. It was used to detect 15 more genetically distinct bornaviruses from Australian pythons that represent a group that is likely to contain a number of novel species.

Author summary

Unlike plants and animals, viruses don't leave fossilised remains that can be used to study their ancient history. Rarely, however, some virus sequences end up as integrated copies in host genomes. These 'fossilised' virus sequences provide a window into virus evolution

Funding: The authors received no specific funding for this work.

Competing interests: The authors have declared that no competing interests exist.

on a geological time scale. In this study, we identified bornaviruses in pythons, some of which had neurological disease. Bornaviruses have been associated with persistent neurological infections in a variety of mammalian and avian hosts. Here, we reveal that bornaviruses are associated with similar disease in non-avian reptiles as well. These new snake viruses turned out to be most closely related to bornavirus-like sequences that integrated into the DNA of mammals prior to the major extinction event at the end of the age of dinosaurs, the end-Cretaceous (K-Pg) extinction, 66 million years ago, allowing us to infer details of their prehistoric evolutionary history and origin. We also developed a test to detect these viruses from samples collected from live snakes, and used it to identify more related snake bornaviruses, indicating that this group will likely continue to expand.

Introduction

Bornaviruses are enveloped viruses with single stranded, negative sense, non-segmented, RNA genomes classified to the family *Bornaviridae* in the order *Mononegavirales* [1]. The bornaviral genome is approximately 8,900 nucleotides and is organised into six open reading frames (ORFs): 3'-N (nucleoprotein)-P (phosphoprotein)-X (accessory protein)-M (matrix protein)-G (glycoprotein)-L (RNA-dependent RNA polymerase)-5' [1]. The P and X ORFs overlap; as do M and G [1-4]. Alternative transcription start and stop sites and splicing produce mRNAs that are translated to produce the viral encoded proteins [5-7].

The prototypic bornavirus, Borna disease virus (originally BDV, now BoDV-1), was first detected in horses and sheep [8] but since then, a number of animal hosts have been found to be susceptible to bornavirus infection including rabbits, guinea pigs, macaques, chickens, quail, parrots, canaries, geese, ducks and swans [3, 4, 9-14]. For some time, it was thought that only "warm-blooded" animals (birds and mammals) were susceptible to bornavirus infection [7, 15]. Recent studies have shown that bornaviruses can also infect non-avian reptiles. In 2004, a transcriptome from a Gaboon viper venom gland (*Bitis gabonica*) was reported [16] that contained bornavirus-like sequences [17, 18]. In 2014, a coding complete genome of a bornavirus was recovered from banked frozen tissue from a wild-caught Loveridge's garter snake (*Elapsoidea loveridgei*), but no clinical or other data was associated with this sequence [19]. The host specificity, association with disease, zoonotic potential, and prevalence of these reptile bornaviruses is totally unknown.

Recommendations for how to taxonomically classify bornaviruses were recently suggested by Kuhn et al. [20] and these have largely been adopted by the International Committee on Taxonomy of Viruses (ICTV) [21]. Concordantly, *Bornaviridae* currently consists of a single genus, *Bornavirus*, which contains eight species: the type species, *Mammalian 1 bornavirus* (formerly *Borna disease virus*); *Mammalian 2 bornavirus*; a snake bornavirus species, *Elapid 1 bornavirus*; and five avian bornavirus species, *Passeriform 1 bornavirus*, *Passeriform 2 bornavirus*, *Psittaciform 1 bornavirus*, *Psittaciform 2 bornavirus*, and *Waterbird 1 bornavirus*.

Endogenous bornavirus-like elements (EBLs) are the result of integration of bornavirus RNA (most likely mRNA) into the host cell's genomic DNA. This process is probably mediated by long interspersed nuclear elements-1 (LINE-1) retrotransposons [22, 23]. If integration occurs in a germ cell, an EBL can, over time, become fixed in a population. These EBLs then become "fossilised" remnants of ancient infections, and provide rare but informative phylogenetic signals with which to study RNA virus evolution. EBLs have been described in a number of vertebrate and invertebrate genomes [17, 22, 23], including in snake genomes [24]. It is estimated that endogenous bornavirus-like N fragments 1 and 2 (EBLN1-2) integrated into the

genomes of six species of viper (from *Crotalus* and *Agkistrodon*) approximately 13 million years ago [24]. In some hosts, the integration of EBLs is estimated to have taken place as long ago as 83.3 million years [25]. The predicted nucleoprotein amino acid sequences of endogenous and exogenous bornaviruses have been compared phylogenetically [17, 24]. EBL-encoded proteins and PIWI-interacting RNAs (piRNA) have been associated with functional roles in antiviral defense and cell cycle progression [25–30]. EBLs are significantly more diverse than known extant bornaviruses, so many EBLs have been presumed to be remnants of extinct bornavirus lineages.

In this study, we characterise the genomes of two bornaviruses from Australian carpet pythons (*Morelia spilota*) with neurological disease. These genomes have features typical of bornaviruses, but have a rearranged gene order that sets them apart from other bornaviruses and mononegaviruses in general. These new bornaviruses are highly divergent, forming a distinct lineage from known extant bornaviruses, and are in fact more closely related to EBLs in a number of mammalian genomes. Using phylogenetic analyses calibrated to fossil records and host-virus cophylogenies, we were able to date the divergence of extant bornavirus lineages prior to the end-Cretaceous extinction, 66 MYA. Overall, these findings expand the known genetic diversity, and host and geographical range of bornaviruses, and shed additional light on the ancient evolutionary history of this group of viruses.

Results

Genome and proteome analyses

We used metagenomic sequencing to assemble the coding complete genomes of two distinct bornaviruses from two carpet pythons with neurological disease. The mean coverage for the two genome assemblies was 120 (Carpet python 1, Jungle carpet python virus, JCPV) and 152 (Carpet python 2, Southwest carpet python virus, SWCPV) (Fig 1). The JCPV and SWCPV genomes have six open reading frames (ORFs) larger than 250 nucleotides in the predicted coding orientation (Fig 2). As in other bornavirus genomes, some of the ORFs are partially overlapping. The ORFs encode predicted proteins that correspond to the six major bornavirus proteins but are in the order: 3'-N-X-P-G-M-L-5'. This gene order differs from that of previously described bornaviruses (N-X-P-M-G-L), with the position of the G and M genes being swapped. The genome assemblies of JCPV and SWCPV contain 93 and 71 nt of predicted non-coding region at their 3' ends and 50 and 77 nt at their 5' ends, respectively.

We identified putative transcription initiation and termination sites in the JCPV and SWCPV genomes (Fig 2). The consensus sequence of the predicted transcription termination sites in the JCPV and SWCPV genomes is UAA[A/G]AAA (antigenomic 5'-to-3' orientation) (Fig 3). These termination sites are located at the ends of the predicted N, G, and L coding sequences (CDS) as well as within the L CDS. To identify possible transcription initiation sites, we used the MEME software and an approach similar to that used to identify transcription initiation and termination motifs in nyamiviruses [31, 32]. We identified a shared motif with consensus sequence CCGAA[A/C][A/C]A that may represent transcription initiation sites upstream of the predicted N, X, and M start codons (Fig 3). Transcription from JCPV and SWCPV genome templates is predicted to produce at least 3 or 4 mRNAs (Fig 2B). Although we did not identify evidence of polyadenylation in NGS reads, other bornaviruses and mononegaviruses produce capped, polyadenylated mRNAs, thus we presume that these mRNAs are capped and polyadenylated. We did not find evidence for mRNA splicing in our NGS datasets.

The first ORF in JCPV and SWCPV encodes the predicted viral N proteins, which are 370 (JCPV) and 371 (SWCPV) amino acids (AA), a length within the range of other bornavirus N proteins (369–379 AA). The JCPV and SWCPV N proteins share a 79% pairwise global amino

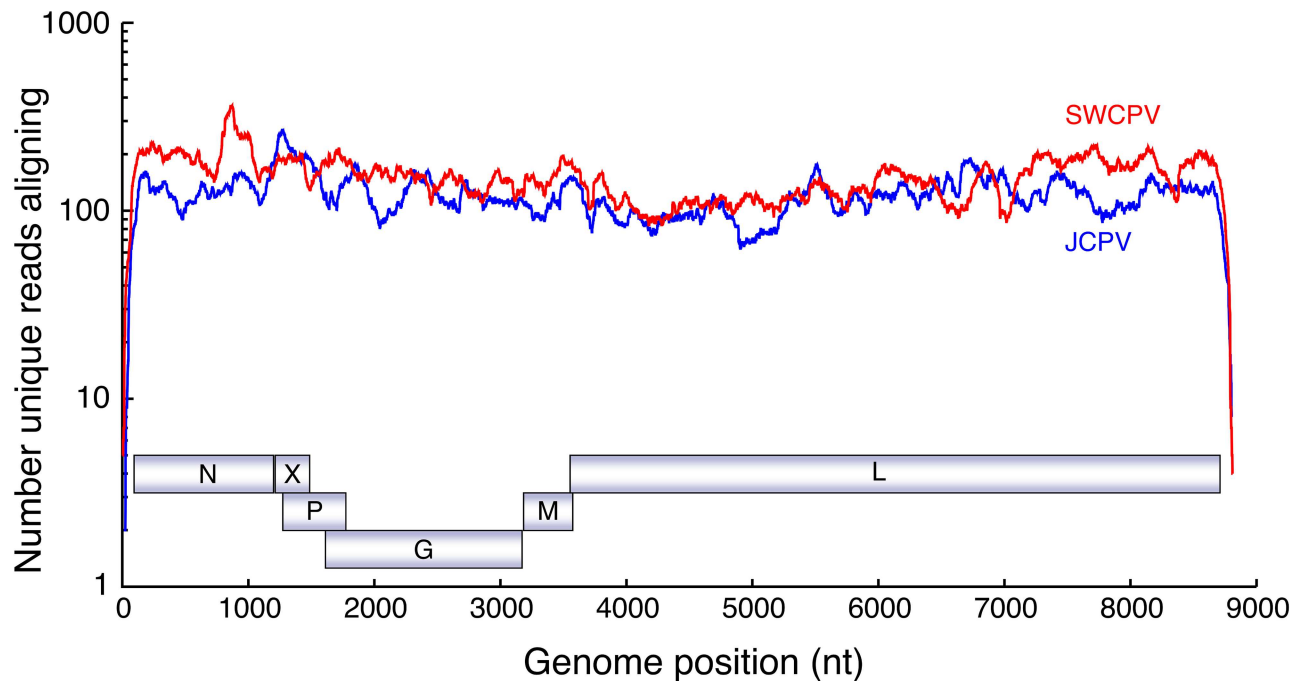


Fig 1. Coverage depth for JCPV and SWCPV genome assemblies. Individual Illumina reads were aligned to the JCPV and SWCPV genome sequences using the Bowtie2 aligner. The number of unique, quality-filtered reads aligning at each base (the coverage) is indicated. Positions of predicted JCPV coding regions are indicated.

<https://doi.org/10.1371/journal.ppat.1006881.g001>

acid identity with each other, 31–45% with endogenous N sequences in mammal genomes, and 17–20% with the N proteins of other bornaviruses (S1 Fig).

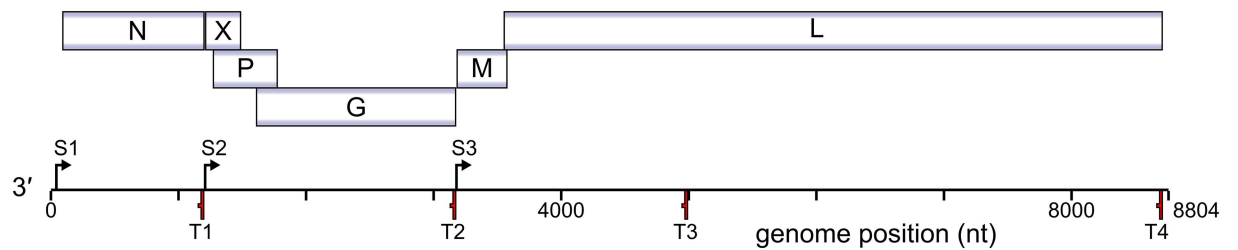
The second ORF in JCPV and SWCPV is predicted to encode the viral X protein of 91 (JCPV) and 92 (SWCPV) AA, respectively, which is nearly the same length as the X protein of other bornaviruses, which range from 86–89 AA. JCPV and SWCPV X are 55% identical and possess low but detectable (15–23%) sequence identity with other bornavirus X proteins (S2 Fig).

The third ORF in JCPV and SWCPV may encode the functional equivalent of the phosphoprotein of other bornaviruses. At 167 and 170 AA, respectively, these putative Ps are slightly shorter than the P proteins of other bornaviruses (~200 AA). JCPV and SWCPV P share 74% pairwise amino acid identity and 15–20% with other bornavirus P proteins (S3 Fig).

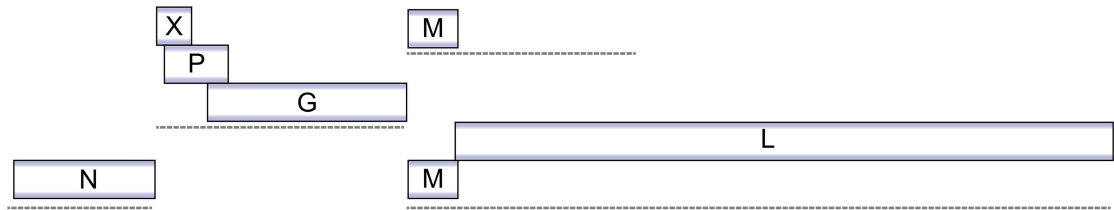
Open reading frames 4–6 in JCPV and SWCPV encode the predicted G, M, and L of these viruses. These homolog assignments were based on predicted sequence and structural similarity (S4–S6 Figs). The predicted G proteins of JCPV and SWCPV are 76% identical and share 25–29% identity with other bornaviruses, and the top hits from a BLASTP search of the NCBI nr database were to bornavirus G proteins (E values < 1×10^{-40}). The predicted M proteins of JCPV and SWCPV are 81% identical and share 22–25% identity with the M of other bornaviruses. The top hit from an hhpred search using JCPV and SWCPV predicted M sequences as queries was to the BDV M protein [E-value 3.5×10^{-4} [33, 34]]. The predicted L proteins of JCPV and SWCPV share 76% pairwise amino acid identity and ~35% with the L proteins of other bornaviruses, making them the most conserved bornavirus proteins.

A number of functionally relevant features have been identified in bornavirus proteins, including nuclear localization and export signals, signal peptides, transmembrane domains, protein-protein interaction domains, and glycosylation sites. We inspected multiple sequence

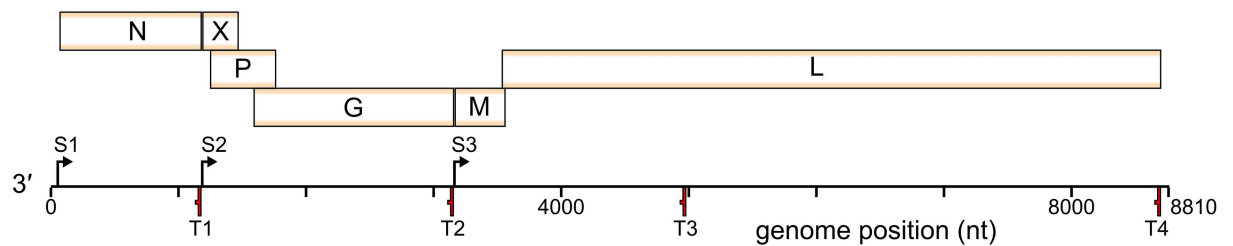
A Jungle carpet python virus (JCPV; MF135780)



B



C Southwest carpet python virus (SWCPV; MF135781)



D Loveridge's garter snake virus 1 (LGSV-1; NC_024778)

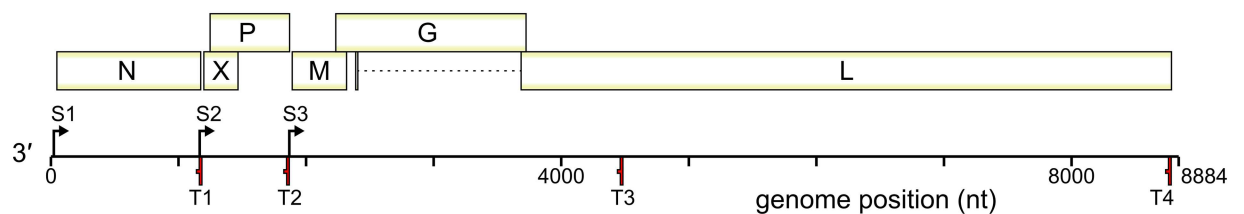


Fig 2. Genome structure and predicted transcriptional map of reptile bornaviruses. (A) to-scale cartoon showing genomic organization of JCPV, including predicted genes and transcriptional start (S) and termination (T) sites. (B) Major predicted transcription products from JCPV genome. (C,D) cartoons of SWCPV and LGSV-1 as in (A).

<https://doi.org/10.1371/journal.ppat.1006881.g002>

alignments of JCPV, SWCPV, and other bornavirus proteins to look for conserved functional motifs. The degree of sequence similarity between JCPV and SWCPV and other bornavirus protein sequences is low, and in most cases, functionally characterized protein motifs were not obviously conserved (S1–S6 Figs). We therefore also analysed protein sequences using a suite of analysis tools to identify putative functional motifs de novo.

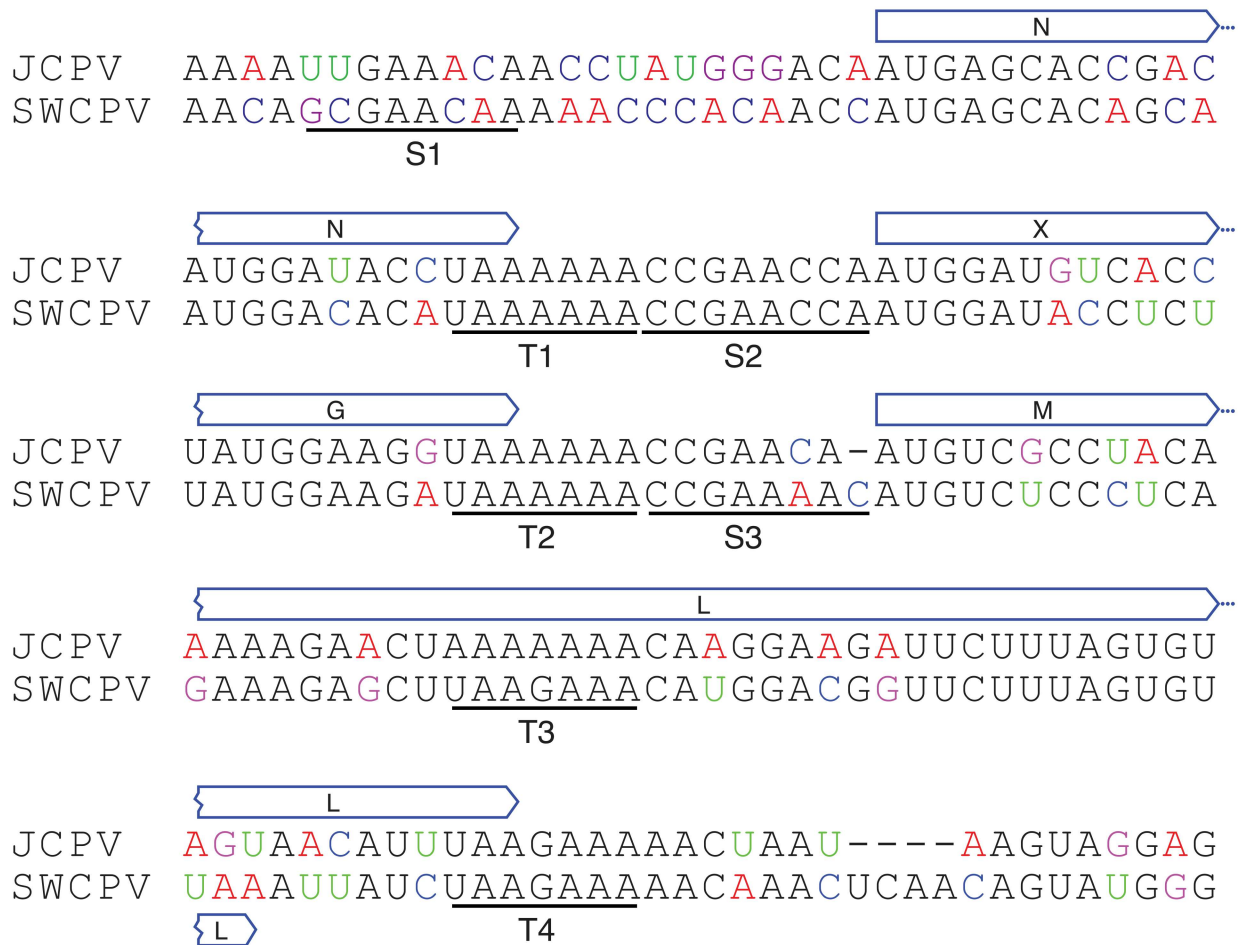


Fig 3. Predicted transcription initiation and termination sites in JCPV and SWCPV genomes. Predicted transcription start (S1-S3) and termination/polyadenylation (T1-T4) signal sites in the JCPV and SWCPV genomes are shown, as are the positions of flanking open reading frames. Sequences are shown in the antigenomic 5'-to-3' orientation.

<https://doi.org/10.1371/journal.ppat.1006881.g003>

As in other bornaviruses, the G proteins of JCPV and SWCPV contained predicted signal peptides, transmembrane domains, and glycosylation sites [6, 35]. Signal peptides were identified near the C-termini of JCPV and SWCPV G proteins, with predicted cleavage sites after residues 16 and 20, respectively (S4 Fig) [36]. Transmembrane domains were predicted in JCPV and SWCPV G proteins at residues 492–514 and 493–515, respectively. No other JCPV and SWCPV proteins contained predicted signal peptides or transmembrane domains. Multiple N- and O-linked glycosylation sites were predicted in JCPV and SWCPV G [37].

Nuclear localization and export signals (NLS and NES) are short motifs that direct proteins into and out of the nucleus [38]. Bornaviruses replicate and transcribe their genomes in the nucleus of infected cells [39], and NLS and NES in bornavirus proteins direct the trafficking of bornaviral ribonucleoprotein complexes [40, 41]. NLS have been identified in the BoDV-1 N, P, and X proteins [41–46]. None of these NLS are obviously conserved in the corresponding JCPV and SWCPV proteins (except for X, see below, Fig 4 and S1–S3 Figs), nor did NLSmapper or NLStradamus predict NLS in these regions. However, these tools both predicted a NLS at another position in JCPV and SWCPV P (58-KKIKRKRETT in JCPV P, and 59-KKAKRKREIV in SWCPV P; S3 Fig).

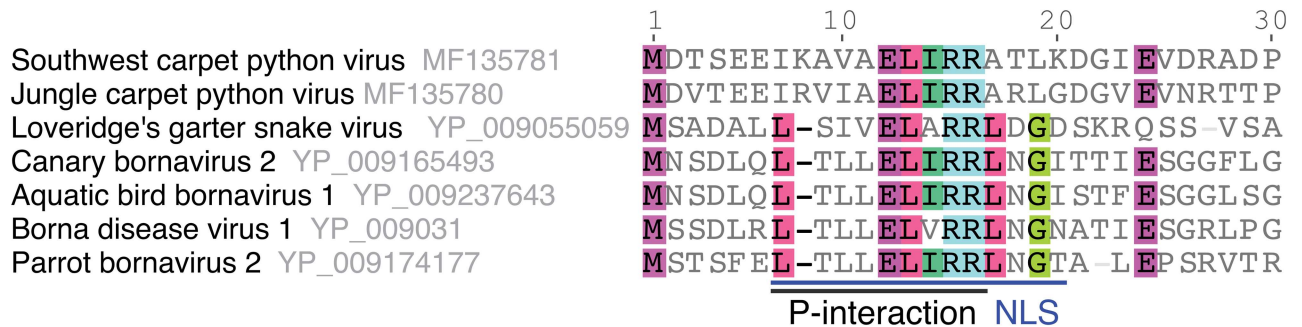


Fig 4. Part of a P-interaction motif is conserved in bornavirus X proteins. A multiple sequence alignment of the putative JCPV and SWCPV X proteins with representative bornavirus X protein sequences. Each virus name is followed by its GenBank accession number. Residues necessary for BoDV-1 X-P interaction and a NLS in BoDV-1 X are highlighted.

<https://doi.org/10.1371/journal.ppat.1006881.g004>

Nuclear export signals have been identified in bornavirus N and P proteins [40, 47]. These sequences are not well conserved in the JCPV and SWCPV N and P proteins (S1 and S2 Figs). A putative NES was predicted by both NESMapper and WREGX at the same location in JCPV and SWCPV P (in JCPV P: V-89-DSIISKIDSLALL; S3 Fig).

A number of domains that mediate the interaction between bornavirus proteins and cellular proteins (e.g. HMGB1) or between bornavirus proteins have been identified [41, 48–52]. For instance, regions in BoDV-1 N and P that mediate their interaction have been identified [48, 50]. These previously identified motifs are for the most part in regions of weak conservation, making it difficult to extrapolate functional relevance (S1 and S3 Figs).

There were; however, some relatively conserved regions in JCPV and SWCPV proteins with possible functional relevance. In the L protein of JCPV and SWCPV, functional motifs that are widely conserved among mononegavirus RNA-dependent RNA polymerases are present (S6 Fig) [53, 54]. The predicted JCPV and SWCPV X proteins share an EL[I/A/V]RR motif with other bornavirus X proteins (Fig 4 and S2 Fig). This region in BoDV-1 X has been implicated in nuclear localization and interaction with P, and it is possible that this domain mediates similar activities in JCPV and SWCPV X [46, 51, 55].

We also identified a possible functional connection between JCPV and SWCPV P and bornavirus P in the form of putative “late domains” near the C-termini of these proteins (Fig 5). Late domains are short peptide motifs found in a variety of viral proteins that mediate interactions with members of cellular endosomal sorting complexes required for transport (ESCRT) machinery to promote budding of enveloped viruses [56, 57]. The putative late domain sequences in the bornavirus proteins are canonical P[S/T]AP and YPXL motifs, except for the P of Loveridge’s garter snake virus-1 [19], which has a YPXL motif, but not a canonical P[S/T]AP sequence (Fig 5). This region in BoDV-1 P has also been identified as being involved in nuclear import (Fig 5 and S3 Fig) [43, 44].

Phylogeny

To place these new viruses phylogenetically, we collected sequences of other bornaviruses and of EBLs. Bayesian phylogenetic trees of the bornaviral N, G, and L genes, and their predicted proteins, are displayed in Figs 6, 7 and 8, respectively. Maximum likelihood (ML) phylogenies were also inferred, and their topologies were essentially identical to Bayesian trees. In all phylogenies, JCPV and SWCPV are most closely related to each other, and next most closely related to a clade of EBL sequences found in various mammalian genomes. In the G analysis, this EBL clade contained only a sole marsupial EBL; in the L analysis, it contained a marsupial

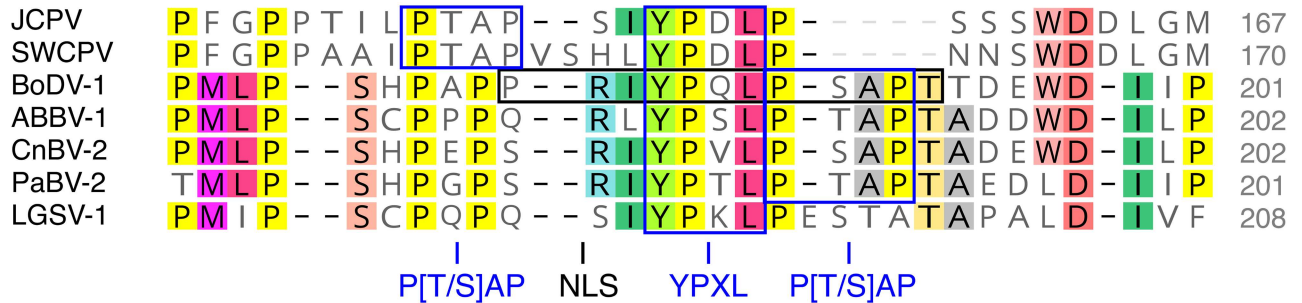


Fig 5. Putative late domain motifs in the C-terminus of bornavirus P proteins. Putative P[S/T]AP and YPXL motifs are indicated in multiple sequence alignments bornavirus P protein sequences. JCPV and SWCPV P were aligned with phylogenetically representative P sequences from the NCBI RefSeq database. Residues conserved in >50% of the sequences are highlighted. Sequence accessions: JCPV: MF135780; SWCPV: MF135781; BoDV-1: NC_001607.1; ABBV-1: NC_029642.1; CnBV-2: NC_027892.1; NC_028106.1; LGSV-1: NC_024778.1. Numbers of C-terminal P residues are indicated.

<https://doi.org/10.1371/journal.ppat.1006881.g005>

and a bat EBL; and in the N analysis, this group had EBLs from marsupials, a bat, and a variety of primates, including humans. In the N and G analyses, a clade containing EBLs from laurasiatherian mammals, aye-aye, and in the N analysis, afrotherian mammals, was the next closest. A lamprey EBL was basal to this group in the N analysis.

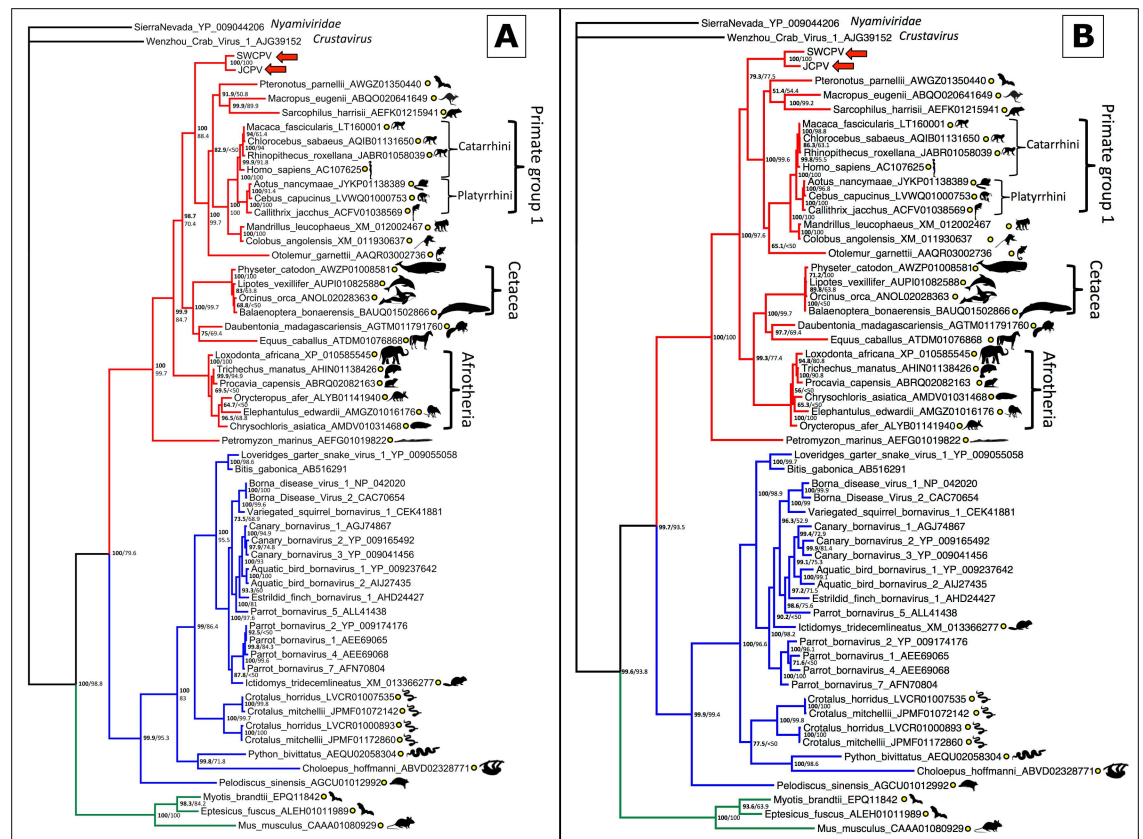


Fig 6. Bayesian phylogenetic tree of MAFFT alignment of homologous bornaviral nucleoprotein (N) amino acid (A) and nucleotide (B) sequences. *Sierra Nevada virus* (GenBank accession # YP_009044206) was used as the outgroup. Confidence of the tree topology is shown by Bayesian posterior probabilities to the left of the slash or above, and maximum likelihood bootstrap values to the right or below. Viruses and EBLs forming a clade with the genus *Bornavirus* are marked in blue, viruses and EBLs clustering with the python bornaviruses are in red, and a third clade of EBLs are in green. Yellow circles indicate EBL sequences.

<https://doi.org/10.1371/journal.ppat.1006881.g006>

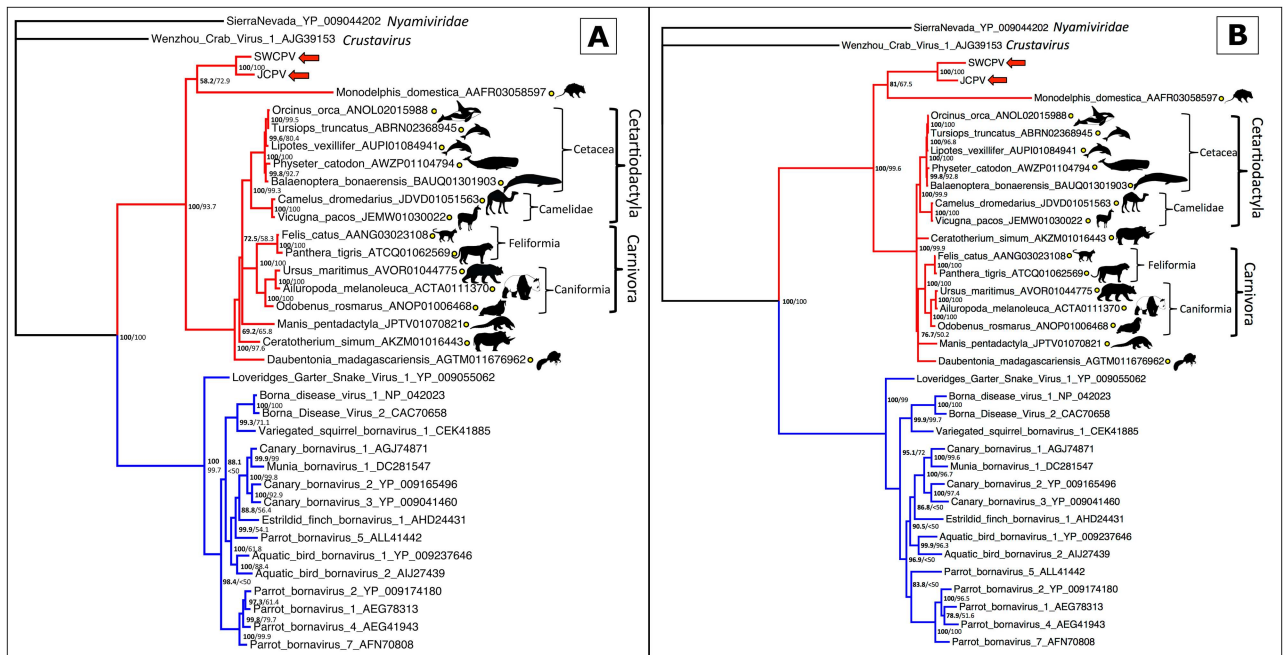


Fig 7. Bayesian phylogenetic tree of MAFFT alignment of homologous bornaviral glycoprotein (G) amino acid (A) and nucleotide (B) sequences. *Sierra Nevada virus* (GenBank accession # YP_009044202) was used as the outgroup. Confidence of the tree topology is shown by Bayesian posterior probabilities to the left of the slash or above, and maximum likelihood bootstrap values to the right or below. Viruses forming a clade with the genus *Bornavirus* are marked in blue, and viruses and EBLs clustering with the python bornaviruses are in red. Yellow circles indicate EBL sequences.

<https://doi.org/10.1371/journal.ppat.1006881.g007>

Using PCR with degenerate primers, 15 distinct bornavirus sequences were detected from 10 other Australian python collections across four Australian states: Queensland, New South Wales, Victoria and Western Australia. From one of these collections (Qld_4), six unique bornavirus sequences were detected from the same species of snake (diamond python, *Morelia spilota spilota*). PCR products were sequenced using Sanger sequencing and phylogenetic analysis of these short L sequences showed diversity was present (Fig 9); however, confidence values for this phylogeny were fairly low.

We next investigated whether the JCPV- and SWCPV-like EBLs were the result of a single integration event into an ancestral mammalian genome or the result of multiple independent integrations. We constructed EBL-host co-phylogenies, and aligned genomic contigs containing EBLs to determine whether EBL integration sites were syntenic. Host-virus/EBL phylogenetic congruence and EBL synteny would be consistent with a single ancestral integration event. We performed these analyses for N- and G-like EBLs.

In host-EBL co-phylogenies, the topologies of the EBL/virus and the host trees were very similar. The predicted N protein analysis found an afrotherian EBL clade with a branching pattern similar to host relationships, a cetacean EBL clade that did not have strong support for branching order, a marsupial EBL clade containing only two members, and a primate clade similar to the branching orders of both platyrrhine and catarrhine primates, including humans (Fig 10). Endogenous bornavirus-like elements from two catarrhine primates, colobus (*Colobus angolensis*) and mandrill (*Mandrillus leucophaeus*), clustered separately. An aye-aye (*Daubentonia madagascariensis*) EBL grouped with EBLs from laurasiatherian mammals, and a bat/marsupial EBL cluster grouped with a primate EBL group, both in discordance with the host branching pattern.

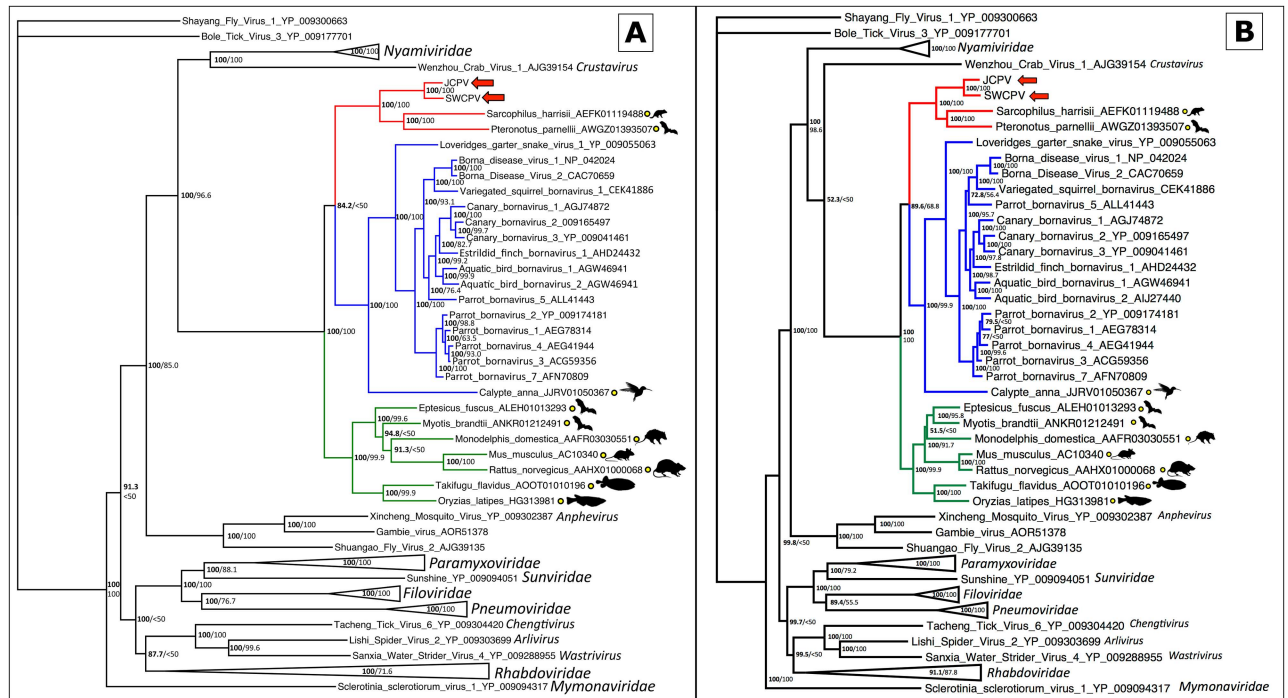


Fig 8. Bayesian phylogenetic tree of MAFPT alignment of homologous bornaviral polymerase (L) amino acid (A) and nucleotide (B) sequences. *Shayang fly virus 1* (GenBank accession # YP_009300663) was used as the outgroup. Confidence of the tree topology is shown by Bayesian posterior probabilities to the left of the slash or above, and maximum likelihood bootstrap values to the right or below. Viruses and EBLs forming a clade with the genus *Bornavirus* are marked in blue, viruses and EBLs clustering with the python bornaviruses are in red, a third clade of EBLs are in green, and non-bornaviral *Mononegavirales* are in black with families collapsed. Yellow circles indicate EBL sequences.

<https://doi.org/10.1371/journal.ppat.1006881.g008>

Synteny was found for the EBLNs within the afrotherian clade, within the cetacean clade, within “primate group 1”, and between the mandrill and colobus monkey contigs (Fig 10). The aye-aye, Parnell’s mustached bat (*Pteronotus parnelli*), tammar wallaby (*Macropus eugenii*), and Antarctic minke whale (*Balaenoptera bonaerensis*) contigs containing EBLNs were all under 3000bp, and were therefore too short to determine whether synteny was present. Multiple conserved frameshifts and stop codons were present within clades of EBL sequences, consistent with an ancestral integration event and a lack of coding capacity preservation.

The predicted G protein analysis found concordance with the host tree of the EBLs (Fig 11). All Laurasiatherian hosts were in concordance.

Looking at the synteny of EBL-containing genome contigs, all EBLGs from laurasiatherian hosts shared a syntenic integration site, consistent with a single integration event (Fig 12). The aye-aye contig containing an EBLG was only 2273bp, and was therefore too short to determine whether synteny was present. Examination of the G alignments also revealed that frameshifts and stop codons were shared within clades, including the presence of a stop codon homologous to amino acid 113 of JCPV in all laurasiatherian EBLs except tigers (*Panthera tigris*) and polar bears (*Ursus maritimus*) (S1 Appendix). Given that domestic cats (*Felis catus*), giant pandas (*Ailuropoda melanoleuca*), and walrus (*Odobenus rosmarus*), as well as cetartiodactyls and white rhinoceros (*Ceratotherium simum*), all have the stop codon, the most parsimonious explanation is that the stop codon was acquired in an early laurasiatherian and lost in tigers and polar bears independently. Synteny was not found between the gray short-tailed opossum (*Monodelphis domestica*) EBLG contig and other EBLG contigs.

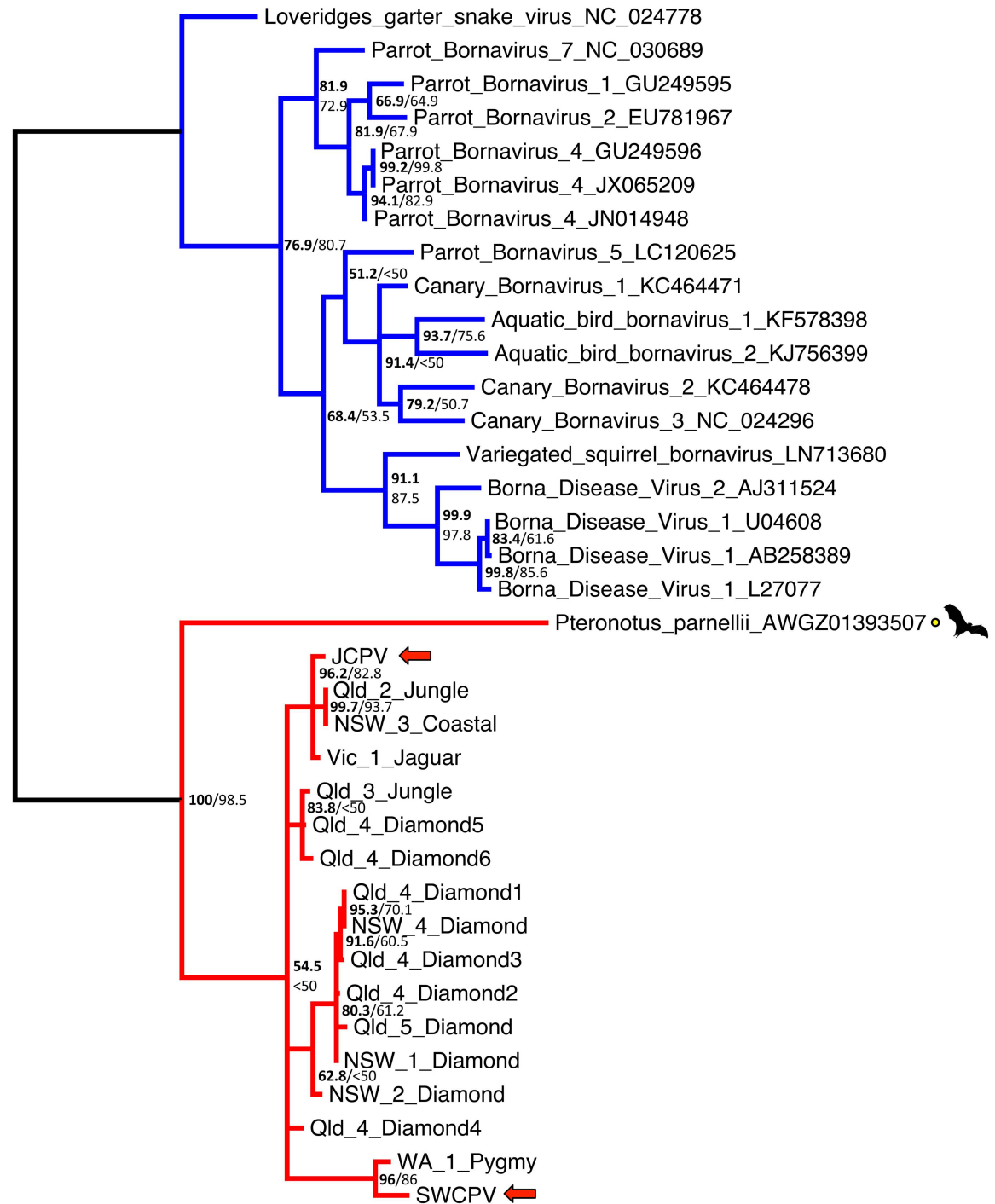


Fig 9. Bayesian phylogenetic tree of MAAFT alignment of homologous bornaviral partial polymerase (L) 211–217 nucleotide sequences. *Loveridge's garter snake virus 1* (GenBank accession # NC_024778) was used as the outgroup. Confidence of the tree topology obtained is shown by Bayesian posterior probabilities to the left of the slash or above, and maximum likelihood bootstrap values are to the right or below. Viruses in the genus *Bornavirus* are marked in blue, and viruses and EBLs clustering with the python bornaviruses are in red. Python bornaviruses are labelled as Australian state, collection number, host species, and animal number. Qld = Queensland, NSW = New South Wales, Vic = Victoria, WA = Western Australia, Jungle = jungle carpet python (*Morelia spilota cheynei*), Coastal = coastal carpet python (*M.s.mcdowelli*), Jaguar = jaguar carpet python (*M.spilota*), Diamond = diamond python (*M.s.spilota*), Pygmy = pygmy python (*Antaresia perthensis*).

<https://doi.org/10.1371/journal.ppat.1006881.g009>

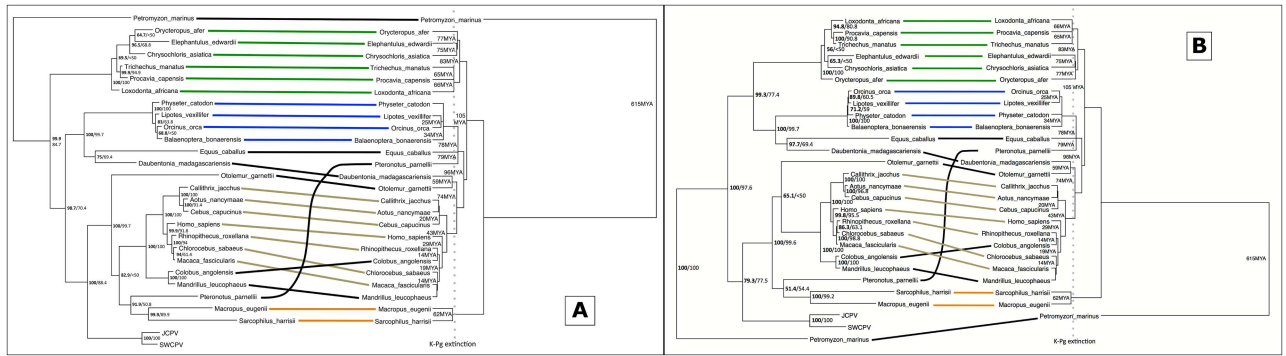


Fig 10. Tanglegram of bornaviral nucleoprotein (N) EBLs (amino acid [A] or nucleotide [B] sequences) and their host species. The nucleoprotein EBL tree is on the left, with confidence of the tree topology obtained shown by Bayesian posterior probabilities to the left of the slash or above, and maximum likelihood bootstrap values to the right or below. The host tree, taken from TimeTree (52), is on the right, and divergence dates in millions of years (MYA) are indicated, with the end-Cretaceous (K-Pg) extinction marked as a dotted line. Connections of an afrotherian clade are marked in green, a cetacean clade are marked in blue, a primate clade are marked in olive, and a marsupial clade are marked in orange.

<https://doi.org/10.1371/journal.ppat.1006881.g010>

We took advantage of the overlapping ORFs in bornavirus genomes to attempt to infer the gene order in the genomes of the viruses whose integration produced the mammalian EBLs most closely related to JCPV and SWCPV. In JCPV and SWCPV, the beginning of the G ORF overlaps with the end of the P ORF (Fig 2). In contrast, in other bornaviruses and mononegaviruses, the beginning of the G ORF overlaps with the end of the M ORF. We inspected the sequences at the beginning of the G ORFs in the EBLGs and found encoded protein sequences in the other 2 reading frames similar to the ends of JCPV and SWCPV P, including a PTAP late domain motif conserved in most of the sequences (Figs 5 and 13). This supports, but does not prove, that the genome of the ancestor virus of JCPV, SWCPV, and the mammalian EBLs contained the atypical N-X-P-G-M-L gene order.

Animals

Of the 27 pythons (*Morelia spilota* and *Antaresia* spp.) that were PCR-positive for reptile bornaviruses and in which tissues were examined histologically, 12 had neurological signs that included progressive caudal paresis, flaccid paralysis, delayed righting reflex and incoordination.

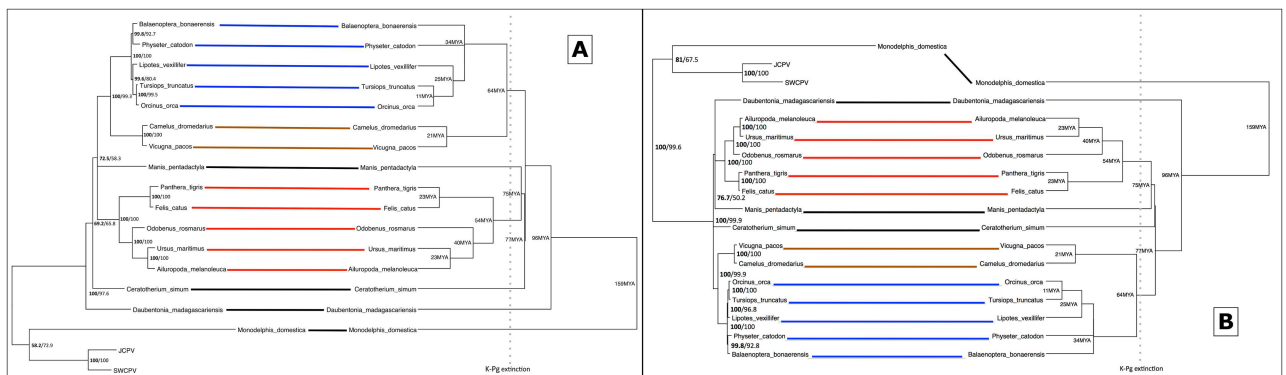


Fig 11. Tanglegram of bornaviral glycoprotein (G) EBLs (amino acid [A] or nucleotide [B] sequences) and their host species. In each panel, The glycoprotein EBL tree is on the left, with confidence of the tree topology obtained shown by Bayesian posterior probabilities to the left of the slash or above, and maximum likelihood bootstrap values to the right or below. The host tree, taken from TimeTree [117], is on the right, and divergence dates in millions of years (MYA) are indicated, with the end-Cretaceous (K-Pg) extinction marked as a dotted line. Connections of a cetacean clade are marked in blue, a camelid clade are marked in brown, and a carnivore clade are marked in red.

<https://doi.org/10.1371/journal.ppat.1006881.g011>

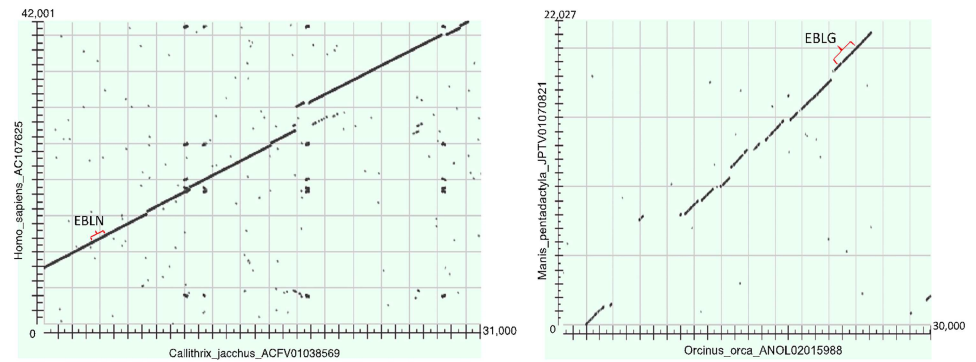


Fig 12. Representative dotplots of genome regions containing endogenous bornavirus-like regions. Human (*Homo sapiens*) vs. marmoset (*Callithrix jacchus*) is shown on the left, with a nucleoprotein EBL marked with a red bracket. Pangolin (*Manis pentadactyla*) vs. orca (*Orcinus orca*) is shown on the right, with a glycoprotein EBL marked with a red bracket. In both cases, the surrounding genome regions also align well, indicating that the EBLs have been introduced into the same site in the two genomes.

<https://doi.org/10.1371/journal.ppat.1006881.g012>

Of these 12, four had mild to moderate nonsuppurative encephalitis characterised by patchy gliosis with variable lymphocytic perivascular cuffing. These four snakes also had mild to moderate lymphocyte infiltration of a few to many peripheral and autonomic nerves and ganglia. Of 15 PCR-positive snakes without neurological signs, two had mild nonsuppurative encephalitis.

Discussion

Here, we describe the identification of novel bornaviruses, jungle carpet python virus (JCPV) and southwest carpet python virus (SWCPV), in Australian carpet pythons with neurological disease. These viruses are more closely related to a clade of ‘fossilised’ endogenous bornavirus sequences than they are to other bornaviruses. Thus, JCPV and SWCPV are the ‘living’ descendants of viruses whose integration millions of years ago into ancestral mammalian genomes gave rise to these EBLs. Three major clades of bornaviruses and EBLs have been described: the first described clade, containing members of the genus *Bornavirus* and EBLs; the JCPV/SWCPV clade; and a third clade of N- and L-like EBLs in mammal and fish genomes (Figs 6 and 8). It is plausible that there are extant bornaviruses in this third clade awaiting discovery.

A taxonomic proposal has been submitted to the International Committee on Taxonomy of Viruses supporting the classification of these viruses into a new genus, within the family

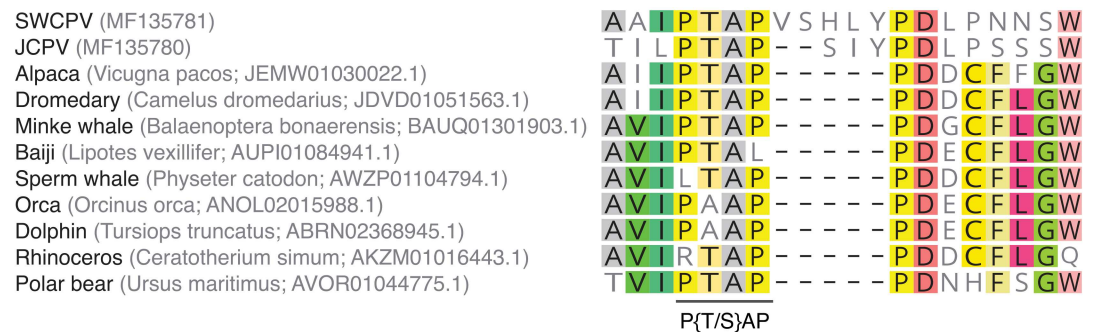


Fig 13. P-like sequences at the beginning of EBLGs. The sequences predicted to be encoded in the other (non G-encoding) reading frames at the beginning of EBLGs were investigated. A motif similar to the end of the JCPV and SWCPV P sequences was identified, consistent with a P-G gene overlap in the virus genomes from which these EBLs derived.

<https://doi.org/10.1371/journal.ppat.1006881.g013>

Bornaviridae (TaxoProp 2017.005M.N.v1.Carbovirus). This will provide impetus to resolve the previously identified issue of whether “bornavirus” refers to a member of the family *Bornaviridae* or the genus *Bornavirus*, which contains all previously identified bornaviruses [20]. Our study also provides some guidance as to how the endogenous bornaviruses could be classified, should the ICTV decide to include them in future taxonomy.

We developed a degenerate PCR to detect JCPV and SWCPV and used it to recover an additional 15 unique sequences of related virus from Australian pythons, indicating that this group is likely to contain a diverse group of novel bornaviruses. We were able to detect viral RNA from oral-cloacal swabs, whole blood and a variety of tissue samples (e.g. brain, lung, liver, kidney, gonad). These primers target a conserved region of the L gene, making this assay suitable for diagnostic testing and bornavirus discovery in a variety of host species (not just snakes) where bornavirus infection is suspected.

The genome organisation of JCPV and SWCPV is in large part similar to the members of the genus *Bornavirus* [1, 6, 58, 59], although the gene order in JCPV and SWCPV is N-X-P-G-M-L, whereas the gene order in the “classic” bornaviruses and in most mononegaviruses is N-X-P-M-G-L [G or other transmembrane glycoprotein(s)]. It is likely that along the lineage leading to JCPV, SWCPV, and the related EBLs a rearrangement occurred that resulted in the transposition of the G and M genes. That this rearrangement was possible is remarkable, given that in both configurations the G gene overlaps significantly with neighbouring ORFs. Gene order is correlated with transcription level and mutation rate in the mononegaviruses, with 5' genes transcribed at lower levels and showing lower mutation rates [60]. The G protein is typically the major antigenic determinant in the *Mononegavirales*; the impact of the altered position on relative gene evolution rates merits future investigation.

Bornaviruses use a variety of mechanisms to produce different mRNA and protein species [1, 6, 58, 61–63]. Initiation and termination of transcription at sites spread through the genome produce monocistronic and polycistronic polyadenylated messages. Additional mRNA species are generated through transcriptional read-through of termination signals and splicing, which enable the translation of downstream ORFs and the production of alternative protein isoforms. Jungle carpet python virus and SWCPV appear to employ a strategy that is generally the same as that used for other bornaviruses to direct the synthesis of viral gene products, as we were able to identify putative transcription initiation and termination sites in their genomes at the expected locations. We did not find evidence for mRNA splicing and could not identify putative splice sites by comparison to other bornaviruses given the high degree of divergence. Nevertheless, it is possible that some of the JCPV and SWCPV mRNAs are spliced. These predictions will have to be validated experimentally once these viruses have been isolated or rescued using reverse genetics.

Dating of ancient viral evolution is problematic. Unlike plants and animals, a fossil record is absent. One approach to estimating viral divergence times has been to calculate rates of change based on isolates from different time points, and to use these rates to predict divergence times of isolates. Using these methods in the order *Mononegavirales*, morbillivirus substitution rates have been estimated to be approximately $6\text{--}7 \times 10^{-4}$ substitutions/site/year, predicting divergence dates less than 2000 years ago in the genus [64]. Rhabdoviral substitution rates have been estimated to be approximately $1\text{--}8 \times 10^{-4}$ substitutions/site/year [65]. Bornaviral N gene divergence rates have been calculated to range from approximately $0.4\text{--}2 \times 10^{-4}$ substitutions/site/year in BoDV-1 to $5\text{--}30 \times 10^{-4}$ substitutions/site/year in avian bornaviruses, with the BoDV-1 most recent common ancestor (MRCA) estimated at 302 years ago and the avian bornavirus MRCA at 772 years ago [66]. However, substitution rates may vary significantly. There is evidence of a 27-fold decrease in substitution rates in persistently infected Ebola virus cases [67].

When virus endogenisation appears to predate host divergence, host divergence times can be used to estimate viral divergence, often resulting in much lower rates than those calculated from virus isolates. Endogenous bornavirus integrations in rattlesnakes have been estimated to be 8–13 million years old [24]. Bats in the genus *Eptesicus* have harboured an endogenous bornavirus-like element for 11.8 million years [54]. Bracoviruses, large double-stranded DNA viruses, have been reported to have coevolved with their insect hosts for 310 million years [68], and retroviruses appear to have codiverged with their vertebrate hosts at least 450 million years ago [69]. The discrepancy between higher short term viral evolutionary rates and lower long-term rates appears to be consistent across diverse viral groups [70]. Short term rates may not account for purifying selection seen over longer time scales; this time dependent rate phenomenon needs to be considered when examining viruses over diverse time scales.

The finding that these novel divergent exogenous bornaviruses cluster with an ancestral laurasiatherian EBLG integration (77MYA) and a previously identified ancestral afrotherian EBLN integration (83 MYA, [25]) argues that these viruses diverged from previously known bornaviruses prior to the end-Cretaceous (K-Pg) extinction 66 million years ago, the major extinction event marking the end of the large dinosaurs.

Physiology and the fossil record make it surprising that mammals dominated after the end-Cretaceous extinction. Therapsida, the lineage of which mammals are the only remaining members, were the dominant clade in the Permian [71]. The largest extinction in the fossil record, the end-Permian extinction 251 million years ago, was a climate warming event due to atmospheric carbon release [72]. Mammalian renal and respiratory physiology results in greater water loss than that of Sauropsida (reptiles, including birds) [73, 74]. In the hot arid environment of the end-Permian extinction, the mammalian ancestors were severely reduced in number and size, and reptiles dominated [75].

There is strong evidence that climate warming played a significant role in the end-Cretaceous extinction [76]. Given the physiological disadvantages mammals have with water conservation, and the previous result of the end-Permian climate warming, it is unexpected that mammals would dominate following an end-Cretaceous climate warming event.

Endogenous viral elements have been shown to protect against infection with similar viruses, including an EBLN in a thirteen-lined ground squirrel (*Ictidomys tridecemlineatus*) that inhibits replication of Borna disease virus [27, 77]. It is possible that the JCPV- and SWCPV-like EBLs block the replication of other members of this clade. EBLs found in the clade containing JCPV and SWCPV, with the exception of the lamprey EBLN, are all from mammalian hosts.

Diverse members of the *Mononegavirales* have been strongly associated with significant population-level impacts on host species: for example, Ebola virus in central African great apes [78], distemper virus in Ethiopian wolves (*Canis simensis*) [79], morbillivirus infection in pilot whales (*Globicephala melas*) [80], and viral haemorrhagic septicaemia virus in Pacific herring (*Clupea pallasii*) [81].

In this study, it was revealed that infection with JCPV or SWCPV is variably associated with neurological signs, and only occasionally with nonsuppurative encephalitis and peripheral ganglioneuritis. The presence of virus in clinically and neurohistologically normal snakes is similar to what has been described in other species that are susceptible to bornavirus infection [7, 82–84]. In birds infected with avian bornaviruses, in some populations and species, there is a relatively good correlation between presence of virus with neuropathology [85, 86], although in others, the correlation is highly variable, with persistent infection in clinically normal birds being common [12, 14, 87–89]. When bornavirus is associated with neuropathology, nonsuppurative encephalitis, as was seen in our cases, is typical [82, 90, 91]. Also, the nonsuppurative encephalitis seen in the present study was usually accompanied by nonsuppurative peripheral

ganglioneuritis; as has been described in birds [83, 85, 86]. Therefore, while these preliminary results suggest that JCPV and SWCPV have an association with disease in pythons, further work is needed to describe a number of fundamental aspects of these viral infections, including epidemiological and controlled infection studies to investigate disease causality and the mechanisms of viral transmission.

The zoonotic potential of bornaviruses remains unclear. Avian bornaviruses (ABV) are not known to naturally infect mammals [92], and ABV genotypes 2 and 4 could not be grown in three mammalian cell lines [93]. There has long been controversy regarding the association of BoDV-1 with human neuropsychiatric disorders [82, 84, 94, 95]. However, in light of the recent association between fatal neurological disease in people and variegated squirrel bornavirus 1 infection that plausibly was acquired from squirrels [96], the zoonotic potential of these novel bornaviruses from pythons should also be examined, though no data exist to suggest that these viruses can infect mammals.

Disease due to bornavirus infection appears to most significantly impact the surviving dinosaurs, the birds. Psittacine bornaviruses have a significant negative impact on populations of the critically endangered Spix's macaw (*Cyanopsitta spixii*) [97]. The extant Dinosauria appear to have relatively fewer endogenous viruses than mammals, and endogenous bornaviruses appear to be 6 to 13-fold less common in bird genomes than mammals [98]. Endogenous bornaviruses do not show deep relationships within the Dinosauria; one survey of 48 avian genomes found that only three had endogenous bornavirus-like elements, and all three appeared to have independent integration sites and not share ancestry [98]. The prehistoric clinical significance of the JCPV/SWCPV clade of viruses is not known, but protection from bornaviral disease by EBLs could have provided a selective advantage to mammals following the end-Cretaceous extinction.

Materials and methods

Ethics statement

Tissue samples from snakes were used in this study. These snakes were humanely euthanased by the attending veterinarians (listed in the acknowledgements section) on humane grounds and due to their poor prognoses. Tissue samples were submitted to the corresponding author and it was only after a number of investigations, were the novel viruses discovered that are described in this manuscript. The decision was then made to disseminate this information by way of publication. For the snakes that were sampled live, they were sampled for the primary purpose of diagnostic screening. This means that the snakes were sampled independent of this study. However, the information obtained from this diagnostic testing was then used for this manuscript. In short, no animal was used for the primary purpose of this study. Animals were sampled and tested for diagnostic purposes so that the attending veterinarian could better manage the snake collections they were working with.

Animals

In 2013, an adult jungle carpet python (*Morelia spilota cheynei* = Carpet python 1) from a zoological park in Queensland, Australia, was euthanased for ongoing and progressive signs of neurological disease that did not respond to supportive care. In 2014, a male 3.5 year old south-west carpet python (*Morelia spilota imbricata* = Carpet python 2) from a private collection in Western Australia, was euthanased for ongoing inappetence, lethargy and a decreased righting reflex. Fresh frozen brain, lung and spleen from Carpet python 1, and fresh frozen brain from Carpet python 2, were submitted for molecular testing of viruses at Murdoch University, Australia. Once PCR testing was developed to screen for reptile bornaviruses (see

elsewhere), other infected pythons were identified through the diagnostic laboratory of one of the authors (THH). All snake samples used in this study were primarily analysed for diagnostic purposes, as per the request of the veterinarians attending to the health of these animals, and who submitted the samples for diagnostic testing. All the veterinarians who submitted samples that were subsequently used in this study were aware that their samples could be used for research purposes.

Nucleic acid extraction

The three tissue samples from Carpet python 1 were pooled together. Nucleic acid was extracted from tissues using the MELT Total Nucleic Acid Isolation System (cat. no. AM1983, Ambion, Thermo Fisher, Victoria, Australia) following the manufacturer's recommendations. During the extraction from the pooled tissue homogenate from Carpet python 1, the optional DNase treatment step was included. Extracted nucleic acid from Carpet python 2 was treated with DNase using the TURBO DNA-free Kit (cat. no. AM1907, Ambion, Thermo Fisher, Victoria, Australia) following the manufacturer's recommendations.

Next generation sequencing and genome analyses

The two DNase-treated total nucleic acid extracts (one from each carpet python) were then depleted of ribosomal RNA (rRNA) using the RiboMinus Eukaryote System v2 (cat. no. A15026, Ambion, Thermo Fisher, Victoria, Australia) following the manufacturer's recommendations. The DNase-treated rRNA-depleted total nucleic acid extracts were then submitted to the Australian Genome Research Facility (www.agrf.org.au) for next-generation sequencing using Illumina HiSeq 2500 (Carpet python 1) and Illumina MiSeq (Carpet python 2). Both sequencing reactions used 150 base pair, paired-end (PE) reads.

De novo assembly of unfiltered sequencing reads into contiguous sequences (contigs) was performed using CLC Genomics (version 8.0.1, QIAGEN). Standard settings for the assembly were used except the Word Size and Bubble Size were set at 64 and 100, respectively. The assembled contigs were used as queries to search for similarities in the NCBI database using BLASTN after limiting the search to virus organisms (taxid: 10239). The nucleotide and predicted amino acid sequences of contigs that had similarities to viral sequences were then used as queries to search the NCBI non-redundant nucleotide and protein databases using BLASTN and BLASTP, respectively. These methods identified contigs corresponding to coding complete bornaviral genomes in each of the two carpet python samples. The sequences of these two genomes were checked for accuracy by mapping the reads to the putative bornaviral genomes using standard settings in CLC Genomics.

The accuracy of these genome sequences was then validated using a second approach that also searched for other possible candidate pathogens. Low quality sequences were trimmed or removed using the Trimmomatic tool, version 0.32 [99], with the following settings: LEADING:20, TRAILING:20, SLIDINGWINDOW:4:25, and MINLEN:40. Then, potential PCR duplicated sequences were collapsed using the CD-HIT-EST tool, version 4.6 [100], with parameter $-c$ 0.96. Remaining reads were assembled using the SPAdes assembler, version 3.5.0 [101], with default parameters. To validate bornavirus assemblies, reads were mapped to draft genome assemblies using Bowtie2, version 2.2.5 [102], with parameters—local—qc-filter—score-min C,120,1. Draft assemblies were corrected and validated by manual inspection in Geneious, version 9.0.4 [103]. Depth of coverage was calculated using SAMTOOLS (htslib) version 1.2.1 [104]. Remaining (non bornavirus) contigs and non-assembling reads were then taxonomically assessed, first by using the BLASTN tool to align to the NCBI nucleotide database. Sequences not producing a nucleotide-level alignment were then searched via translated-

nucleotide to protein alignments against the NCBI non-redundant (nr) protein sequence database using the Rapsearch2 tool, version 2.23, with parameters $-a\ t, -1\ 20,$ and $-e\ 1\ e-2$ [105].

The two genome assembly methods used (CLC Genomics and SPAdes Assembler) produced identical genome sequences. From the tissue homogenate from Carpet python 1, an 8,915 nucleotide contig was assembled that represents a coding complete genome of a bornavirus that we named jungle carpet python virus (JCPV). From the brain homogenate of Carpet python 2, an 8,920 nucleotide contig was assembled that represents a coding complete genome of a second bornavirus that we named southwest carpet python virus (SWCPV). These two genome sequences have been deposited in Genbank under accession numbers MF135780 (JCPV) and MF135781 (SWCPV). Raw sequence data has been deposited in the NCBI Short Read Archive (SRA; accession PRJNA390668).

Homologs of predicted viral protein sequences were identified using BLASTP to search the NCBI (nr) protein database. For sequences that lacked detectable similarity by BLASTP, the HHpred homology detection and structure prediction tool, version 2.0 [106], was also used. To identify endogenous bornavirus-like sequences, the TBLASTN tool was used to search the NCBI genomes database using the predicted bornaviral protein sequences as queries.

We used a variety of tools to perform de novo identification of putative functional features in JCPV and SWCPV genomes and proteins. De novo identification of NLS and NES is prone to false positive predictions [107]. For instance, the NLS in BoDV-1 X resembles a leucine-rich NES more than it does a typical NLS [46]. We therefore used multiple prediction tools and report candidate NES and NLS that were identified at the same positions in both JCPV and SWCPV proteins. We used NLSmapper and NLStradamus to predict NLS, and NESMapper and Wregex to predict NES [107–110]. Transmembrane domains were predicted using the TMHMM2.0 web service [111]. Signal peptides were predicted using the SignalP 4.1 server with the sensitive option enabled [36]. Putative transcription termination sites were predicted based on their genomic location, their conservation in the two new viral genomes, and similarity to well characterised sites in the genomes of other bornaviruses [4, 58, 62]. Transcription start sites were predicted using MEME software (v 4.12.0), using as input to MEME the 20 bases before the predicted N start codons as well as the bases between the poly-A tracts after the N and G ORFs and the predicted start codons of the X and M ORFs [31].

Development of PCR to detect JCPV and SWCPV in clinical samples

A PCR was designed to detect JCPV and SWCPV. Due to the considerable divergence of these viruses from other known bornaviruses, regions of the RNA-dependent RNA polymerase (L) that are highly conserved among bornaviruses were surveyed for suitable primer annealing targets. The primer pair Reptile bornavirus F (RBV-F) 5' GGNATGAGRCARAARYTNTGRAC and RBV-R 5' AARTAYTGYYTTYTTNCCRTAYTCRTA was chosen (S7 Fig). These primers were then tested on oral-cloacal swabs, whole blood and a variety of tissue samples obtained from Australian captive pythons, many of which had neurological signs of disease. Nucleic acid was extracted from oral-cloacal swabs using the Purelink Viral RNA/DNA Mini Kit (cat. no. 12280050, Thermo Fisher) according to the manufacturer's recommendations. For whole blood and tissue samples, the QIAamp *cador* Pathogen Mini Kit (cat. no. 54104, Qiagen) was used. For whole blood, a 2 μ L aliquot was added to 198 μ L of phosphate-buffered saline (PBS, pH 7.4) and then the manufacturer's instructions were followed. For tissue samples, nucleic acid was extracted following the manufacturer's recommendations that included pretreatment method T4. Briefly, segments of tissue with a total volume of $\sim 2\text{--}3\text{ mm}^3$ were homogenised in phenol (pH 8, cat. no. P4557, Sigma) and PBS using a Mini-Beadbeater 24 (cat. no. 112011EUR, Biospec) at 3,000 oscillations per minute for 2 min using 0.5 mL of zirconia/silica

beads (1 mm diameter, cat. no. 11079110z, Biospec). Nucleic acid was eluted into 30 μ L of RNase-free water (swabs) or buffer AVE (blood and tissue). For PCR, 10 μ L of 2 x master mix and 0.8 μ L of RT-Taq enzyme from the Superscript III One-Step RT-PCR System with Platinum *Taq* DNA Polymerase (cat. no. 12574026, Thermo Fisher) were added to RBV-F and RBV-R (1 μ M final concentration for each primer). The total volume was brought to 20 μ L using 1 μ L of extracted nucleic acid and PCR-grade water. Cycling conditions consisted of 50°C x 30min, 94°C x 2min, 15 x (94°C x 20s, 65°C x 30s [decreased by 1°C every cycle], 72°C x 25s), 35 x (94°C x 20s, 50°C x 30s, 72°C x 25s). Ribonucleic acid from JCPV was used as a positive control and a no template extraction was used as a negative control. Amplicons near to the expected size (256 nucleotides) were cut from the gel and sequenced using standard methods. Fifteen unique bornavirus sequences were obtained (GenBank accession numbers MF166903-MF166917) and were included with JCPV and SWCPV in phylogenetic analyses after the primer sequences had been removed.

For 27 Australian pythons that were PCR positive for reptile bornaviruses, a wide range of tissues, including brain, were examined histologically using standard processing techniques and haematoxylin and eosin staining.

Phylogeny

Predicted JCPV and SWCPV N, G, and L amino acid sequences were used in TBLASTN searches of the GenBank database, including the whole genome shotgun contigs (wgs), to look for endogenous bornaviral elements. Endogenous bornaviral elements were examined for potential frameshifts using BLASTX, and amino acid sequences accounting for this were predicted (S1 Appendix). Homologous predicted viral and endogenous amino acid sequences were aligned using MAFFT [112]. Amino acid alignments were then converted back to the nucleotide sequences using PAL2NAL [113]. Sierra Nevada virus, in the *Nyamiviridae*, was used as an outgroup for the N and G analyses. Due to wider conservation, representatives of all the genera of *Mononegavirales* were included in the L analysis, and Shayang fly virus 1 was designated as the outgroup. Bayesian analyses of nucleotide alignments were performed using MrBayes 3.2.6 on the CIPRES server, with a general time reversible (GTR) model and a proportion of invariant sites [114, 115]. The first 25% of 2,000,000 iterations were discarded as a burn in. Maximum likelihood (ML) bootstrap analyses of each alignment were performed using RAxML on the CIPRES server with gamma distributed rate variation and a proportion of invariant sites and a GTR model. Bootstrap analysis was used to test the strength of the ML tree topology, with 1000 subsets [116].

For analysis of additional shorter python bornavirus partial L sequences, homologous 211–217 nucleotide sequences were aligned based on MAFFT alignments of predicted amino acid sequences. Loveridge's garter snake virus 1 was used as an outgroup, and Bayesian and maximum likelihood analyses were performed using a GTR model with the above software.

Host trees with divergence times were obtained from TimeTree [117]. Tanglegrams were generated using Dendroscope 3 [118]. To assess synteny of EBL integration sites in host genomes, TBLASTX comparisons of pairs of sequences were analysed using dot plots.

Supporting information

S1 Fig. Alignment of bornavirus N proteins. JCPV and SWCPV N were aligned with phylogenetically representative N sequences from the NCBI RefSeq database. Predicted and validated functional motifs are indicated (see text). Residues conserved in >50% of the sequences are highlighted. Sequence accessions: JCPV: MF135780; SWCPV: MF135781; BoDV-1: NC_001607.1; ABBV-1: NC_029642.1; CnBV-2: NC_027892.1; NC_028106.1; LGSV-1:

NC_024778.1.
(TIFF)

S2 Fig. Alignment of bornavirus X proteins. JCPV and SWCPV X were aligned with phylogenetically representative X sequences from the NCBI RefSeq database. Predicted and validated functional motifs are indicated (see text). Residues conserved in >50% of the sequences are highlighted. Sequence accessions: JCPV: MF135780; SWCPV: MF135781; BoDV-1: NC_001607.1; ABBV-1: NC_029642.1; CnBV-2: NC_027892.1; NC_028106.1; LGSV-1: NC_024778.1.
(TIFF)

S3 Fig. Alignment of bornavirus P proteins. JCPV and SWCPV P were aligned with phylogenetically representative P sequences from the NCBI RefSeq database. Predicted and validated functional motifs are indicated (see text). Residues conserved in >50% of the sequences are highlighted. Sequence accessions: JCPV: MF135780; SWCPV: MF135781; BoDV-1: NC_001607.1; ABBV-1: NC_029642.1; CnBV-2: NC_027892.1; NC_028106.1; LGSV-1: NC_024778.1.
(TIFF)

S4 Fig. Alignment of bornavirus G proteins. JCPV and SWCPV G were aligned with phylogenetically representative G sequences from the NCBI RefSeq database. Predicted and validated functional motifs are indicated (see text). Residues conserved in >50% of the sequences are highlighted. Sequence accessions: JCPV: MF135780; SWCPV: MF135781; BoDV-1: NC_001607.1; ABBV-1: NC_029642.1; CnBV-2: NC_027892.1; NC_028106.1; LGSV-1: NC_024778.1.
(TIFF)

S5 Fig. Alignment of bornavirus M proteins. JCPV and SWCPV M were aligned with phylogenetically representative M sequences from the NCBI RefSeq database. Predicted and validated functional motifs are indicated (see text). Residues conserved in >50% of the sequences are highlighted. Sequence accessions: JCPV: MF135780; SWCPV: MF135781; BoDV-1: NC_001607.1; ABBV-1: NC_029642.1; CnBV-2: NC_027892.1; NC_028106.1; LGSV-1: NC_024778.1.
(TIFF)

S6 Fig. Conserved motifs in block III of JCPV and SWCPV L proteins. An alignment of the region of bornavirus L and EBLV sequences that includes the conserved A, B, C, and D motifs in Block III that were described in Poch et al. [53]. Residues that were found by Poch et al. [53] to be universally conserved are indicated by stars. Consensus residues shared by >50% of the sequences are highlighted. Sequence accessions: JCPV: MF135780; SWCPV: MF135781; BoDV-1: NC_001607.1; ABBV-1: NC_029642.1; CnBV-2: NC_027892.1; NC_028106.1; LGSV-1: NC_024778.1. Alignment corresponds to residues 337–645 of BoDV-1 L.
(TIFF)

S7 Fig. Primer annealing sites. A multiple sequence alignment of the putative jungle carpet python virus and southwest carpet python virus L proteins with the cognate L protein sequences from seven of the eight species of the genus *Bornavirus*. This area of the genome has not been sequenced in a *Passeriform 2 bornavirus*. Each virus name is followed by its GenBank accession number and columns are labelled relative to the amino acid residue number of Borna disease virus-1 L protein (AAM68151).
(TIFF)

S1 Appendix. Frameshifts of EBLG, EBLL and EBLN with corresponding MAFFT alignments for EBLG and EBLN. EBLG, EBLL and EBLN nucleotide sequences in fasta format followed by amino acid sequences corresponding to frames 1–3.

(ZIP)

Acknowledgments

We are very grateful to Drs Peter Barratt and James Haberfield for providing this study with tissue samples from carpet pythons 1 and 2, respectively. We thank Dr Shane Besier for preliminary histological examinations on two of the snakes.

Author Contributions

Conceptualization: Timothy H. Hyndman, Mark D. Stenglein, James F. X. Wellehan, Jr.

Data curation: Timothy H. Hyndman, Catherine M. Shilton, Mark D. Stenglein, James F. X. Wellehan, Jr.

Formal analysis: Timothy H. Hyndman, Catherine M. Shilton, Mark D. Stenglein, James F. X. Wellehan, Jr.

Investigation: Timothy H. Hyndman, Catherine M. Shilton, Mark D. Stenglein, James F. X. Wellehan, Jr.

Methodology: Timothy H. Hyndman, Catherine M. Shilton, Mark D. Stenglein, James F. X. Wellehan, Jr.

Project administration: Timothy H. Hyndman.

Resources: Timothy H. Hyndman, Mark D. Stenglein, James F. X. Wellehan, Jr.

Software: Timothy H. Hyndman, Mark D. Stenglein, James F. X. Wellehan, Jr.

Validation: Timothy H. Hyndman, Catherine M. Shilton, Mark D. Stenglein, James F. X. Wellehan, Jr.

Visualization: Timothy H. Hyndman, Mark D. Stenglein, James F. X. Wellehan, Jr.

Writing – original draft: Timothy H. Hyndman, Mark D. Stenglein, James F. X. Wellehan, Jr.

Writing – review & editing: Timothy H. Hyndman, Catherine M. Shilton, Mark D. Stenglein, James F. X. Wellehan, Jr.

References

1. Schwemmler M, Carbone K, Tomonago K, Nowotny N, Garten W. Bornaviridae. In: King AM, Adams MJ, Carstens EB, Lefkowitz EJ, editors. *Virus taxonomy: classification and nomenclature of viruses: Ninth Report of the International Committee on Taxonomy of Viruses*. 9. Amsterdam: Elsevier; 2012. p. 658–64.
2. Gancz AY, Kistler AL, Greninger AL, Farnoushi Y, Mechani S, Perl S, et al. Experimental induction of proventricular dilatation disease in cockatiels (*Nymphicus hollandicus*) inoculated with brain homogenates containing avian bornavirus 4. *Virology*. 2009; 6:100. Epub 2009/07/11. <https://doi.org/10.1186/1743-422X-6-100> PMID: 19589169.
3. Honkavuori KS, Shivaprasad HL, Williams BL, Quan PL, Hornig M, Street C, et al. Novel borna virus in psittacine birds with proventricular dilatation disease. *Emerg Infect Dis*. 2008; 14(12):1883–6. Epub 2008/12/03. <https://doi.org/10.3201/eid1412.080984> PMID: 19046511.
4. Kistler AL, Gancz A, Clubb S, Skewes-Cox P, Fischer K, Sorber K, et al. Recovery of divergent avian bornaviruses from cases of proventricular dilatation disease: identification of a candidate etiologic agent. *Virology*. 2008; 5:88. Epub 2008/08/02. <https://doi.org/10.1186/1743-422X-5-88> PMID: 18671869.

5. Schneemann A, Schneider PA, Lamb RA, Lipkin WI. The remarkable coding strategy of borna disease virus: a new member of the nonsegmented negative strand RNA viruses. *Virology*. 1995; 210(1):1–8. Epub 1995/06/20. <https://doi.org/10.1006/viro.1995.1311> PMID: 7793061.
6. Herden C, Briese T, Lipkin WI, Richt JA. Bornaviridae. In: Knipe DM, Howley PM, editors. *Field's Virology*. 6 ed. Philadelphia: Lippincott Williams & Wilkins; 2013. p. 1124–50.
7. Lipkin WI, Briese T, Hornig M. Borna disease virus—Fact and fantasy. *Virus research*. 2011; 162(1):162–72.
8. Wensman JJ. Bornaviruses. In: Munir M, editor. *Mononegaviruses of Veterinary Importance, Volume 1: Pathobiology and Molecular Diagnosis*. 1: CABI; 2013. p. 1.
9. Koprowski H, Lipkin WI. *Borna disease*: Springer-Verlag; 1995.
10. Ludwig H, Kraft W, Kao M, Gosztonyi G, Dahme E, Krey H. [Borna virus infection (Borna disease) in naturally and experimentally infected animals: its significance for research and practice]. *Tierärztliche Praxis*. 1984; 13(4):421–53.
11. Weissenböck H, Sekulin K, Bakonyi T, Högl S, Nowotny N. Novel avian bornavirus in a nonpsittacine species (canary; *Serinus canaria*) with enteric ganglioneuritis and encephalitis. *Journal of virology*. 2009; 83(21):11367–71. <https://doi.org/10.1128/JVI.01343-09> PMID: 19706702
12. Payne S, Covalada L, Jianhua G, Swafford S, Baroch J, Ferro PJ, et al. Detection and characterization of a distinct bornavirus lineage from healthy Canada geese (*Branta canadensis*). *Journal of virology*. 2011; 85(22):12053–6. <https://doi.org/10.1128/JVI.05700-11> PMID: 21900161
13. Guo J, Shivaprasad H, Rech RR, Heatley JJ, Tizard I, Payne S. Characterization of a new genotype of avian bornavirus from wild ducks. *Virology journal*. 2014; 11(1):1.
14. Guo J, Covalada L, Heatley JJ, Baroch JA, Tizard I, Payne SL. Widespread avian bornavirus infection in mute swans in the Northeast United States. 2012.
15. Hornig M, Briese T, Lipkin WI. Borna disease virus. *Journal of neurovirology*. 2003; 9(2):259–73. <https://doi.org/10.1080/13550280390194064> PMID: 12707857
16. Francischetti IM, My-Pham V, Harrison J, Garfield MK, Ribeiro JM. Bitis gabonica (Gaboon viper) snake venom gland: toward a catalog for the full-length transcripts (cDNA) and proteins. *Gene*. 2004; 337:55–69. <https://doi.org/10.1016/j.gene.2004.03.024> PMID: 15276202
17. Horie M, Honda T, Suzuki Y, Kobayashi Y, Daito T, Oshida T, et al. Endogenous non-retroviral RNA virus elements in mammalian genomes. *Nature*. 2010; 463(7277):84–7. Epub 2010/01/08. <https://doi.org/10.1038/nature08695> PMID: 20054395.
18. Fujino K, Horie M, Honda T, Nakamura S, Matsumoto Y, Francischetti IM, et al. Evolutionarily conserved interaction between the phosphoproteins and X proteins of bornaviruses from different vertebrate species. *PloS one*. 2012; 7(12):e51161. Epub 2012/12/14. <https://doi.org/10.1371/journal.pone.0051161> PMID: 23236446.
19. Stenglein MD, Leavitt EB, Abramovitch MA, McGuire JA, DeRisi JL. Genome sequence of a bornavirus recovered from an African garter snake (*Elapsoidea loveridgei*). *Genome announcements*. 2014; 2(5):e00779–14. <https://doi.org/10.1128/genomeA.00779-14> PMID: 25301640
20. Kuhn JH, Durrwald R, Bao Y, Briese T, Carbone K, Clawson AN, et al. Taxonomic reorganization of the family Bornaviridae. *Arch Virol*. 2015; 160(2):621–32. Epub 2014/12/03. <https://doi.org/10.1007/s00705-014-2276-z> PMID: 25449305.
21. ICTV. *Virus Taxonomy*: 2016 Release 2017 [25th July 2017]. <http://www.ictvonline.org/virusTaxonomy.asp>.
22. Horie M, Kobayashi Y, Suzuki Y, Tomonaga K. Comprehensive analysis of endogenous bornavirus-like elements in eukaryote genomes. *Phil Trans R Soc B*. 2013; 368(1626):20120499. <https://doi.org/10.1098/rstb.2012.0499> PMID: 23938751
23. Belyi VA, Levine AJ, Skalka AM. Unexpected inheritance: multiple integrations of ancient bornavirus and ebolavirus/marburgvirus sequences in vertebrate genomes. *PLoS Pathog*. 2010; 6(7):e1001030. <https://doi.org/10.1371/journal.ppat.1001030> PMID: 20686665
24. Gilbert C, Meik J, Dashevsky D, Card D, Castoe T, Schaack S. Endogenous hepadnaviruses, bornaviruses and circoviruses in snakes. *Proceedings of the Royal Society of London B: Biological Sciences*. 2014; 281(1791):20141122.
25. Kobayashi Y, Horie M, Nakano A, Murata K, Itou T, Suzuki Y. Exaptation of Bornavirus-Like Nucleoprotein Elements in Afrotherians. *PLoS Pathog*. 2016; 12(8):e1005785. <https://doi.org/10.1371/journal.ppat.1005785> PMID: 27518265
26. He P, Sun L, Zhu D, Zhang H, Zhang L, Guo Y, et al. Knock-Down of Endogenous Bornavirus-Like Nucleoprotein 1 Inhibits Cell Growth and Induces Apoptosis in Human Oligodendroglia Cells. *International journal of molecular sciences*. 2016; 17(4):435. Epub 2016/03/31. <https://doi.org/10.3390/ijms17040435> PMID: 27023521.

27. Fujino K, Horie M, Honda T, Merriman DK, Tomonaga K. Inhibition of Borna disease virus replication by an endogenous bornavirus-like element in the ground squirrel genome. *Proceedings of the National Academy of Sciences of the United States of America*. 2014; 111(36):13175–80. Epub 2014/08/27. <https://doi.org/10.1073/pnas.1407046111> PMID: 25157155.
28. Honda T, Tomonaga K. Endogenous non-retroviral RNA virus elements evidence a novel type of antiviral immunity. *Mobile genetic elements*. 2016; 6(3):e1165785. Epub 2016/08/12. <https://doi.org/10.1080/2159256X.2016.1165785> PMID: 27510928.
29. Parrish NF, Fujino K, Shiromoto Y, Iwasaki YW, Ha H, Xing J, et al. piRNAs derived from ancient viral processed pseudogenes as transgenerational sequence-specific immune memory in mammals. *RNA (New York, NY)*. 2015; 21(10):1691–703. Epub 2015/08/19. <https://doi.org/10.1261/rna.052092.115> PMID: 26283688.
30. Sofuku K, Parrish NF, Honda T, Tomonaga K. Transcription Profiling Demonstrates Epigenetic Control of Non-retroviral RNA Virus-Derived Elements in the Human Genome. *Cell reports*. 2015; 12(10):1548–54. Epub 2015/09/01. <https://doi.org/10.1016/j.celrep.2015.08.007> PMID: 26321645.
31. Bailey TL, Boden M, Buske FA, Frith M, Grant CE, Clementi L, et al. MEME SUITE: tools for motif discovery and searching. *Nucleic acids research*. 2009; 37(Web Server issue):W202–8. Epub 2009/05/22. <https://doi.org/10.1093/nar/gkp335> PMID: 19458158.
32. Mihindukulasuriya KA, Nguyen NL, Wu G, Huang HV, da Rosa APT, Popov VL, et al. Nyamanini and midway viruses define a novel taxon of RNA viruses in the order Mononegavirales. *Journal of virology*. 2009; 83(10):5109–16. <https://doi.org/10.1128/JVI.02667-08> PMID: 19279111
33. Hildebrand A, Remmert M, Biegert A, Soding J. Fast and accurate automatic structure prediction with HHpred. *Proteins*. 2009; 77 Suppl 9:128–32. Epub 2009/07/25. <https://doi.org/10.1002/prot.22499> PMID: 19626712.
34. Neumann P, Lieber D, Meyer S, Dautel P, Kerth A, Kraus I, et al. Crystal structure of the Borna disease virus matrix protein (BDV-M) reveals ssRNA binding properties. *Proceedings of the National Academy of Sciences of the United States of America*. 2009; 106(10):3710–5. Epub 2009/02/25. <https://doi.org/10.1073/pnas.0808101106> PMID: 19237566.
35. Schneider PA, Hatalski CG, Lewis AJ, Lipkin WI. Biochemical and functional analysis of the Borna disease virus G protein. *J Virol*. 1997; 71(1):331–6. Epub 1997/01/01. PMID: 8985354.
36. Petersen TN, Brunak S, von Heijne G, Nielsen H. SignalP 4.0: discriminating signal peptides from transmembrane regions. *Nature methods*. 2011; 8(10):785–6. Epub 2011/10/01. <https://doi.org/10.1038/nmeth.1701> PMID: 21959131.
37. Steentoft C, Vakhrushev SY, Joshi HJ, Kong Y, Vester-Christensen MB, Schjoldager KT, et al. Precision mapping of the human O-GalNAc glycoproteome through SimpleCell technology. *The EMBO journal*. 2013; 32(10):1478–88. Epub 2013/04/16. <https://doi.org/10.1038/emboj.2013.79> PMID: 23584533.
38. Nakielny S, Dreyfuss G. Transport of proteins and RNAs in and out of the nucleus. *Cell*. 1999; 99(7):677–90. Epub 2000/01/05. PMID: 10619422
39. Briese T, de la Torre JC, Lewis A, Ludwig H, Lipkin WI. Borna disease virus, a negative-strand RNA virus, transcribes in the nucleus of infected cells. *Proceedings of the National Academy of Sciences of the United States of America*. 1992; 89(23):11486–9. Epub 1992/12/01. PMID: 1454837.
40. Kobayashi T, Kamitani W, Zhang G, Watanabe M, Tomonaga K, Ikuta K. Borna disease virus nucleoprotein requires both nuclear localization and export activities for viral nucleocytoplasmic shuttling. *J Virol*. 2001; 75(7):3404–12. Epub 2001/03/10. <https://doi.org/10.1128/JVI.75.7.3404-3412.2001> PMID: 11238866.
41. Honda T, Tomonaga K. Nucleocytoplasmic shuttling of viral proteins in borna disease virus infection. *Viruses*. 2013; 5(8):1978–90. Epub 2013/08/24. <https://doi.org/10.3390/v5081978> PMID: 23965528.
42. Pyper JM, Gartner AE. Molecular basis for the differential subcellular localization of the 38- and 39-kilodalton structural proteins of Borna disease virus. *J Virol*. 1997; 71(7):5133–9. Epub 1997/07/01. PMID: 9188580.
43. Shoya Y, Kobayashi T, Koda T, Ikuta K, Kakinuma M, Kishi M. Two proline-rich nuclear localization signals in the amino- and carboxyl-terminal regions of the Borna disease virus phosphoprotein. *J Virol*. 1998; 72(12):9755–62. Epub 1998/11/13. PMID: 9811710.
44. Schwemmle M, Jehle C, Shoemaker T, Lipkin WI. Characterization of the major nuclear localization signal of the Borna disease virus phosphoprotein. *The Journal of general virology*. 1999; 80 (Pt 1):97–100. Epub 1999/02/06. <https://doi.org/10.1099/0022-1317-80-1-97> PMID: 9934690.
45. Kobayashi T, Shoya Y, Koda T, Takashima I, Lai PK, Ikuta K, et al. Nuclear targeting activity associated with the amino terminal region of the Borna disease virus nucleoprotein. *Virology*. 1998; 243(1):188–97. Epub 1998/04/07. <https://doi.org/10.1006/viro.1998.9049> PMID: 9527928.

46. Wolff T, Unterstab G, Heins G, Richt JA, Kann M. Characterization of an unusual importin alpha binding motif in the borna disease virus p10 protein that directs nuclear import. *The Journal of biological chemistry*. 2002; 277(14):12151–7. Epub 2002/01/18. <https://doi.org/10.1074/jbc.M109103200> PMID: 11796712.
47. Yanai H, Kobayashi T, Hayashi Y, Watanabe Y, Ohtaki N, Zhang G, et al. A methionine-rich domain mediates CRM1-dependent nuclear export activity of Borna disease virus phosphoprotein. *J Virol*. 2006; 80(3):1121–9. Epub 2006/01/18. <https://doi.org/10.1128/JVI.80.3.1121-1129.2006> PMID: 16414989.
48. Berg M, Ehrenborg C, Blomberg J, Pipkorn R, Berg AL. Two domains of the Borna disease virus p40 protein are required for interaction with the p23 protein. *The Journal of general virology*. 1998; 79 (Pt 12):2957–63. Epub 1999/01/08. <https://doi.org/10.1099/0022-1317-79-12-2957> PMID: 9880009.
49. Zhang G, Kobayashi T, Kamitani W, Komoto S, Yamashita M, Baba S, et al. Borna disease virus phosphoprotein represses p53-mediated transcriptional activity by interference with HMGB1. *J Virol*. 2003; 77(22):12243–51. Epub 2003/10/29. <https://doi.org/10.1128/JVI.77.22.12243-12251.2003> PMID: 14581561.
50. Schwemmler M, Salvatore M, Shi L, Richt J, Lee CH, Lipkin WI. Interactions of the borna disease virus P, N, and X proteins and their functional implications. *The Journal of biological chemistry*. 1998; 273 (15):9007–12. Epub 1998/05/16. PMID: 9535888.
51. Wolff T, Pflieger R, Wehner T, Reinhardt J, Richt JA. A short leucine-rich sequence in the Borna disease virus p10 protein mediates association with the viral phospho- and nucleoproteins. *The Journal of general virology*. 2000; 81(Pt 4):939–47. Epub 2000/03/22. <https://doi.org/10.1099/0022-1317-81-4-939> PMID: 10725419.
52. Chase G, Mayer D, Hildebrand A, Frank R, Hayashi Y, Tomonaga K, et al. Borna disease virus matrix protein is an integral component of the viral ribonucleoprotein complex that does not interfere with polymerase activity. *J Virol*. 2007; 81(2):743–9. Epub 2006/11/03. <https://doi.org/10.1128/JVI.01351-06> PMID: 17079312.
53. Poch O, Blumberg BM, Bougueleret L, Tordo N. Sequence comparison of five polymerases (L proteins) of unsegmented negative-strand RNA viruses: theoretical assignment of functional domains. *The Journal of general virology*. 1990; 71 (Pt 5):1153–62. Epub 1990/05/01. <https://doi.org/10.1099/0022-1317-71-5-1153> PMID: 2161049.
54. Horie M, Kobayashi Y, Honda T, Fujino K, Akasaka T, Kohl C, et al. An RNA-dependent RNA polymerase gene in bat genomes derived from an ancient negative-strand RNA virus. *Sci Rep*. 2016; 6:25873. Epub 2016/05/14. <https://doi.org/10.1038/srep25873> PMID: 27174689.
55. Malik TH, Kishi M, Lai PK. Characterization of the P protein-binding domain on the 10-kilodalton protein of Borna disease virus. *J Virol*. 2000; 74(7):3413–7. Epub 2000/03/09. PMID: 10708460.
56. Demirov DG, Freed EO. Retrovirus budding. *Virus Res*. 2004; 106(2):87–102. Epub 2004/11/30. <https://doi.org/10.1016/j.virusres.2004.08.007> PMID: 15567490.
57. Zhadina M, Bieniasz PD. Functional interchangeability of late domains, late domain cofactors and ubiquitin in viral budding. *PLoS Pathog*. 2010; 6(10):e1001153. Epub 2010/10/27. <https://doi.org/10.1371/journal.ppat.1001153> PMID: 20975941.
58. Cubitt B, Oldstone C, de la Torre JC. Sequence and genome organization of Borna disease virus. *J Virol*. 1994; 68(3):1382–96. Epub 1994/03/01. PMID: 7906311.
59. Briese T, Schneemann A, Lewis AJ, Park YS, Kim S, Ludwig H, et al. Genomic organization of Borna disease virus. *Proceedings of the National Academy of Sciences of the United States of America*. 1994; 91(10):4362–6. Epub 1994/05/10. PMID: 8183914.
60. Pagan I, Holmes EC, Simon-Loriere E. Level of gene expression is a major determinant of protein evolution in the viral order Mononegavirales. *J Virol*. 2012; 86(9):5253–63. Epub 2012/02/22. <https://doi.org/10.1128/JVI.06050-11> PMID: 22345453.
61. de la Torre JC. Molecular biology of Borna disease virus and persistence. *Frontiers in bioscience: a journal and virtual library*. 2002; 7:d569–79. Epub 2002/01/30. PMID: 11815302.
62. Schneemann A, Schneider PA, Kim S, Lipkin WI. Identification of signal sequences that control transcription of borna disease virus, a nonsegmented, negative-strand RNA virus. *J Virol*. 1994; 68 (10):6514–22. Epub 1994/10/01. PMID: 8083989.
63. Schneider PA, Schneemann A, Lipkin WI. RNA splicing in Borna disease virus, a nonsegmented, negative-strand RNA virus. *J Virol*. 1994; 68(8):5007–12. Epub 1994/08/01. PMID: 8035500.
64. Furuse Y, Suzuki A, Oshitani H. Origin of measles virus: divergence from rinderpest virus between the 11 th and 12 th centuries. *Virology journal*. 2010; 7(1):52.

65. He M, Ding N-Z, He C-Q, Yan X-C, Teng C-B. Dating the divergence of the infectious hematopoietic necrosis virus. *Infection, Genetics and Evolution*. 2013; 18:145–50. <https://doi.org/10.1016/j.meegid.2013.05.014> PMID: 23722020
66. He M, An T-Z, Teng C-B. Evolution of mammalian and avian bornaviruses. *Molecular phylogenetics and evolution*. 2014; 79:385–91. <https://doi.org/10.1016/j.ympev.2014.07.006> PMID: 25046276
67. Blackley DJ, Wiley MR, Ladner JT, Fallah M, Lo T, Gilbert ML, et al. Reduced evolutionary rate in reemerged Ebola virus transmission chains. *Sci Adv*. 2016; 2(4):e1600378. Epub 2016/07/08. <https://doi.org/10.1126/sciadv.1600378> PMID: 27386513.
68. Theze J, Bezier A, Periquet G, Drezzen JM, Herniou EA. Paleozoic origin of insect large dsDNA viruses. *Proceedings of the National Academy of Sciences of the United States of America*. 2011; 108(38):15931–5. Epub 2011/09/14. <https://doi.org/10.1073/pnas.1105580108> PMID: 21911395.
69. Aiewsakun P, Katzourakis A. Marine origin of retroviruses in the early Palaeozoic Era. *Nature communications*. 2017; 8:13954. Epub 2017/01/11. <https://doi.org/10.1038/ncomms13954> PMID: 28071651.
70. Aiewsakun P, Katzourakis A. Time-Dependent Rate Phenomenon in Viruses. *Journal of Virology*. 2016; 90(16):7184–95. Epub 2016/06/03. <https://doi.org/10.1128/JVI.00593-16> PMID: 27252529.
71. Irmis RB, Whiteside JH. Delayed recovery of non-marine tetrapods after the end-Permian mass extinction tracks global carbon cycle. *Proceedings Biological sciences*. 2012; 279(1732):1310–8. Epub 2011/10/28. <https://doi.org/10.1098/rspb.2011.1895> PMID: 22031757.
72. Joachimski MM, Lai X, Shen S, Jiang H, Luo G, Chen B, et al. Climate warming in the latest Permian and the Permian–Triassic mass extinction. *Geology*. 2012; 40(3):195–8.
73. Campbell JW, Vorhaben JE, Smith DD Jr. Uricotely: its nature and origin during the evolution of tetrapod vertebrates. *The Journal of experimental zoology*. 1987; 243(3):349–63. Epub 1987/09/01. <https://doi.org/10.1002/jez.1402430302> PMID: 2890702.
74. Farmer CG. Similarity of Crocodylian and Avian Lungs Indicates Unidirectional Flow Is Ancestral for Archosaurs. *Integrative and comparative biology*. 2015; 55(6):962–71. Epub 2015/07/05. <https://doi.org/10.1093/icb/icc078> PMID: 26141868.
75. Farmer CG. The Evolution of Unidirectional Pulmonary Airflow. *Physiology (Bethesda, Md)*. 2015; 30(4):260–72. Epub 2015/07/03. <https://doi.org/10.1152/physiol.00056.2014> PMID: 26136540.
76. Petersen SV, Dutton A, Lohmann KC. End-Cretaceous extinction in Antarctica linked to both Deccan volcanism and meteorite impact via climate change. *Nature communications*. 2016; 7:12079. Epub 2016/07/06. <https://doi.org/10.1038/ncomms12079> PMID: 27377632.
77. Feschotte C, Gilbert C. Endogenous viruses: insights into viral evolution and impact on host biology. *Nature reviews Genetics*. 2012; 13(4):283–96. Epub 2012/03/17. <https://doi.org/10.1038/nrg3199> PMID: 22421730.
78. Leroy EM, Rouquet P, Formenty P, Souquiere S, Kilbourne A, Froment JM, et al. Multiple Ebola virus transmission events and rapid decline of central African wildlife. *Science (New York, NY)*. 2004; 303(5656):387–90. Epub 2004/01/17. <https://doi.org/10.1126/science.1092528> PMID: 14726594.
79. Gordon CH, Banyard AC, Hussein A, Laurenson MK, Malcolm JR, Marino J, et al. Canine distemper in endangered Ethiopian wolves. *Emerg Infect Dis*. 2015; 21(5):824–32. Epub 2015/04/22. <https://doi.org/10.3201/eid2105.141920> PMID: 25898177.
80. Verborgh P, Gauffier P, Esteban R, Gimenez J, Canadas A, Salazar-Sierra JM, et al. Conservation Status of Long-Finned Pilot Whales, *Globicephala melas*, in the Mediterranean Sea. *Advances in marine biology*. 2016; 75:173–203. Epub 2016/10/25. <https://doi.org/10.1016/bs.amb.2016.07.004> PMID: 27770984.
81. Marty GD, Li TJQ, Carpenter G, Meyers TR, Willits NH. Role of disease in abundance of a Pacific herring (*Clupea pallasii*) population. *Canadian Journal of Fisheries and Aquatic Sciences*. 2003; 60(10):1258–65.
82. Staeheli P, Sauder C, Hausmann J, Ehrensperger F, Schwemmler M. Epidemiology of Borna disease virus. *The Journal of general virology*. 2000; 81(Pt 9):2123–35. Epub 2000/08/22. <https://doi.org/10.1099/0022-1317-81-9-2123> PMID: 10950968.
83. Staeheli P, Rinder M, Kaspers B. Avian bornavirus associated with fatal disease in psittacine birds. *J Virol*. 2010; 84(13):6269–75. Epub 2010/03/12. <https://doi.org/10.1128/JVI.02567-09> PMID: 20219910.
84. Richt JA, Pfeuffer I, Christ M, Frese K, Bechter K, Herzog S. Borna disease virus infection in animals and humans. *Emerg Infect Dis*. 1997; 3(3):343–52. Epub 1997/07/01. <https://doi.org/10.3201/eid0303.970311> PMID: 9284379.
85. Raghav R, Taylor M, Delay J, Ojkic D, Pearl DL, Kistler AL, et al. Avian bornavirus is present in many tissues of psittacine birds with histopathologic evidence of proventricular dilatation disease. *Journal of veterinary diagnostic investigation: official publication of the American Association of Veterinary*

- Laboratory Diagnosticians, Inc. 2010; 22(4):495–508. Epub 2010/07/14. <https://doi.org/10.1177/104063871002200402> PMID: 20622218.
86. Delnatte P, Ojkic D, Delay J, Campbell D, Crawshaw G, Smith DA. Pathology and diagnosis of avian bornavirus infection in wild Canada geese (*Branta canadensis*), trumpeter swans (*Cygnus buccinator*) and mute swans (*Cygnus olor*) in Canada: a retrospective study. *Avian pathology: journal of the WVPA*. 2013; 42(2):114–28. Epub 2013/04/16. <https://doi.org/10.1080/03079457.2013.769669> PMID: 23581438.
 87. Lierz M, Hafez HM, Honkavuori KS, Gruber AD, Olias P, Abdelwhab EM, et al. Anatomical distribution of avian bornavirus in parrots, its occurrence in clinically healthy birds and ABV-antibody detection. *Avian pathology: journal of the WVPA*. 2009; 38(6):491–6. Epub 2009/11/26. <https://doi.org/10.1080/03079450903349238> PMID: 19937538.
 88. Heffels-Redmann U, Enderlein D, Herzog S, Piepenbring A, Bürkle M, Neumann D, et al. Follow-up investigations on different courses of natural avian bornavirus infections in psittacines. *Avian diseases*. 2012; 56(1):153–9. <https://doi.org/10.1637/9844-062811-Reg.1> PMID: 22545541
 89. Villanueva I, Gray P, Mirhosseini N, Payne S, Hoppes S, Honkavuori KS, et al. The diagnosis of proventricular dilatation disease: use of a Western blot assay to detect antibodies against avian Borna virus. *Veterinary Microbiology*. 2010; 143(2–4):196–201. Epub 2009/12/29. <https://doi.org/10.1016/j.vetmic.2009.11.041> PMID: 20036080.
 90. Gosztonyi G, Ludwig H. Borna disease of horses. An immunohistological and virological study of naturally infected animals. *Acta neuropathologica*. 1984; 64(3):213–21. Epub 1984/01/01. PMID: 6437125.
 91. Stitz L, Bilzer T, Planz O. The immunopathogenesis of Borna disease virus infection. *Frontiers in bio-science: a journal and virtual library*. 2002; 7:d541–55. Epub 2002/01/30. PMID: 11815301.
 92. Payne SL, Delnatte P, Guo J, Heatley JJ, Tizard I, Smith DA. Birds and bornaviruses. *Animal health research reviews*. 2012; 13(2):145–56. Epub 2012/12/21. <https://doi.org/10.1017/S1466252312000205> PMID: 23253163.
 93. Rinder M, Ackermann A, Kempf H, Kaspers B, Korbel R, Staeheli P. Broad tissue and cell tropism of avian bornavirus in parrots with proventricular dilatation disease. *J Virol*. 2009; 83(11):5401–7. Epub 2009/03/20. <https://doi.org/10.1128/JVI.00133-09> PMID: 19297496.
 94. Chalmers R, Thomas DR, Salmon R. Borna disease virus and the evidence for human pathogenicity: a systematic review. *Qjm*. 2005; 98(4):255–74. <https://doi.org/10.1093/qjmed/hci039> PMID: 15760926
 95. Hornig M, Briese T, Licinio J, Khabbaz RF, Altshuler LL, Potkin SG, et al. Absence of evidence for bornavirus infection in schizophrenia, bipolar disorder and major depressive disorder. *Molecular psychiatry*. 2012; 17(5):486–93. Epub 2012/02/01. <https://doi.org/10.1038/mp.2011.179> PMID: 22290118.
 96. Hoffmann B, Tappe D, Hoper D, Herden C, Boldt A, Mawrin C, et al. A Variegated Squirrel Bornavirus Associated with Fatal Human Encephalitis. *The New England journal of medicine*. 2015; 373(2):154–62. <https://doi.org/10.1056/NEJMoa1415627> PMID: 26154788.
 97. Hammer S, Watson R. The challenge of managing Spix Macaws (*Cyanopsitta spixii*) at Qatar—an eleven-year retrospective. *Der Zoologische Garten*. 2012; 81(2):81–95.
 98. Cui J, Zhao W, Huang Z, Jarvis ED, Gilbert MT, Walker PJ, et al. Low frequency of paleoviral infiltration across the avian phylogeny. *Genome biology*. 2014; 15(12):539. Epub 2014/12/17. <https://doi.org/10.1186/s13059-014-0539-3> PMID: 25496498.
 99. Bolger AM, Lohse M, Usadel B. Trimmomatic: a flexible trimmer for Illumina sequence data. *Bioinformatics (Oxford, England)*. 2014; 30(15):2114–20. Epub 2014/04/04. <https://doi.org/10.1093/bioinformatics/btu170> PMID: 24695404.
 100. Fu L, Niu B, Zhu Z, Wu S, Li W. CD-HIT: accelerated for clustering the next-generation sequencing data. *Bioinformatics (Oxford, England)*. 2012; 28(23):3150–2. Epub 2012/10/13. <https://doi.org/10.1093/bioinformatics/bts565> PMID: 23060610.
 101. Bankevich A, Nurk S, Antipov D, Gurevich AA, Dvorkin M, Kulikov AS, et al. SPAdes: a new genome assembly algorithm and its applications to single-cell sequencing. *Journal of computational biology: a journal of computational molecular cell biology*. 2012; 19(5):455–77. Epub 2012/04/18. <https://doi.org/10.1089/cmb.2012.0021> PMID: 22506599.
 102. Langmead B, Salzberg SL. Fast gapped-read alignment with Bowtie 2. *Nature methods*. 2012; 9(4):357–9. Epub 2012/03/06. <https://doi.org/10.1038/nmeth.1923> PMID: 22388286.
 103. Kearse M, Moir R, Wilson A, Stones-Havas S, Cheung M, Sturrock S, et al. Geneious Basic: an integrated and extendable desktop software platform for the organization and analysis of sequence data. *Bioinformatics (Oxford, England)*. 2012; 28(12):1647–9. Epub 2012/05/01. <https://doi.org/10.1093/bioinformatics/bts199> PMID: 22543367.

104. Li H, Handsaker B, Wysoker A, Fennell T, Ruan J, Homer N, et al. The Sequence Alignment/Map format and SAMtools. *Bioinformatics* (Oxford, England). 2009; 25(16):2078–9. Epub 2009/06/10. <https://doi.org/10.1093/bioinformatics/btp352> PMID: 19505943.
105. Zhao Y, Tang H, Ye Y. RAPSearch2: a fast and memory-efficient protein similarity search tool for next-generation sequencing data. *Bioinformatics* (Oxford, England). 2012; 28(1):125–6.
106. Soding J, Biegert A, Lupas AN. The HHpred interactive server for protein homology detection and structure prediction. *Nucleic acids research*. 2005; 33(Web Server issue):W244–8. Epub 2005/06/28. <https://doi.org/10.1093/nar/gki408> PMID: 15980461.
107. Kosugi S, Yanagawa H, Terauchi R, Tabata S. NESmapper: accurate prediction of leucine-rich nuclear export signals using activity-based profiles. *PLoS computational biology*. 2014; 10(9): e1003841. Epub 2014/09/19. <https://doi.org/10.1371/journal.pcbi.1003841> PMID: 25233087.
108. Kosugi S, Hasebe M, Tomita M, Yanagawa H. Systematic identification of cell cycle-dependent yeast nucleocytoplasmic shuttling proteins by prediction of composite motifs. *Proceedings of the National Academy of Sciences of the United States of America*. 2009; 106(25):10171–6. Epub 2009/06/13. <https://doi.org/10.1073/pnas.0900604106> PMID: 19520826.
109. Nguyen Ba AN, Pogoutse A, Provart N, Moses AM. NLStradamus: a simple Hidden Markov Model for nuclear localization signal prediction. *BMC Bioinformatics*. 2009; 10:202. Epub 2009/07/01. <https://doi.org/10.1186/1471-2105-10-202> PMID: 19563654.
110. Prieto G, Fullaondo A, Rodriguez JA. Prediction of nuclear export signals using weighted regular expressions (Wregex). *Bioinformatics* (Oxford, England). 2014; 30(9):1220–7. Epub 2014/01/15. <https://doi.org/10.1093/bioinformatics/btu016> PMID: 24413524.
111. Krogh A, Larsson B, von Heijne G, Sonnhammer EL. Predicting transmembrane protein topology with a hidden Markov model: application to complete genomes. *Journal of molecular biology*. 2001; 305(3):567–80. Epub 2001/01/12. <https://doi.org/10.1006/jmbi.2000.4315> PMID: 11152613.
112. Katoh K, Toh H. Improved accuracy of multiple ncRNA alignment by incorporating structural information into a MAFFT-based framework. *BMC bioinformatics*. 2008; 9(1):212.
113. Suyama M, Torrents D, Bork P. PAL2NAL: robust conversion of protein sequence alignments into the corresponding codon alignments. *Nucleic acids research*. 2006; 34(Web Server issue):W609–12. Epub 2006/07/18. <https://doi.org/10.1093/nar/gkl315> PMID: 16845082.
114. Miller MA, Schwartz T, Pickett BE, He S, Klem EB, Scheuermann RH, et al. A RESTful API for access to phylogenetic tools via the CIPRES science gateway. *Evolutionary Bioinformatics*. 2015; 11:43.
115. Ronquist F, Huelsenbeck JP. MrBayes 3: Bayesian phylogenetic inference under mixed models. *Bioinformatics* (Oxford, England). 2003; 19(12):1572–4.
116. Felsenstein J. Confidence limits on phylogenies: an approach using the bootstrap. *Evolution*. 1985:783–91. <https://doi.org/10.1111/j.1558-5646.1985.tb00420.x> PMID: 28561359
117. Hedges SB, Dudley J, Kumar S. TimeTree: a public knowledge-base of divergence times among organisms. *Bioinformatics* (Oxford, England). 2006; 22(23):2971–2.
118. Huson DH, Scornavacca C. Dendroscope 3: an interactive tool for rooted phylogenetic trees and networks. *Systematic biology*. 2012; 61(6):1061–7. <https://doi.org/10.1093/sysbio/sys062> PMID: 22780991